# Vertical Handoff Decision Algorithms for Providing Optimized Performance in Heterogeneous Wireless Networks

SuKyoung Lee, Kotikalapudi Sriram, Kyungsoo Kim, JongHyup Lee, Yoon Hyuk Kim, and Nada Golmie

*Abstract*— **There are currently a large variety of wireless access networks, including the emerging Vehicular Ad hoc Networks (VANETs). A large variety of applications utilizing these networks will demand features such as real-time, high-availability and even instantaneous high-bandwidth in some cases. Therefore, it is imperative for network service providers to make the best possible use of the combined resources of available heterogeneous networks (WLAN, UMTS, VANETs, Wi-MAX, etc.) for connection support. When connections need to migrate between heterogeneous networks for performance and high-availability reasons, seamless vertical handoff is a necessary first step. In the near future, vehicular and other mobile applications will expect seamless vertical handoff between heterogeneous access networks. With regard to vertical handoff performance, there is a critical need for developing algorithms for connection management and optimal resource allocation for seamless mobility. In this paper, we develop a vertical handoff decision algorithm that enables a wireless access network to not only balance the overall load among all attachment points (e.g., Base Stations (BSs) and Access Points (APs)) but also to maximize the collective battery lifetime of Mobile Nodes (MNs). In addition, when ad hoc mode is applied to 3/4G wireless data networks, VANETs and IEEE 802.11 WLANs for more seamless integration of heterogeneous wireless networks, we devise a route selection algorithm to forward data packets to the most appropriate attachment point in order to maximize the collective battery lifetime as well as maintain load balancing. Results based on a detailed performance evaluation study are also presented here to demonstrate the efficacy of the proposed algorithms.**

*Index Terms*— **Mobility management, Intersystem handover, QoS management, Simulation modeling, Seamless mobility, High-availability, VANET, WLAN, Wi-MAX, Vertical handoff, Load balancing.**

## I. Introduction

Connection handoff is no longer limited to migration between two subnets in Wireless Local Area Network (WLAN), or between two cells in a cellular network, generally known as "horizontal handoff". In addition to roaming and horizontal handoff within homogeneous subnets (e.g., consisting only 802.11 WLANs or only cellular networks), supporting service continuity and Quality of Service (QoS) requires seamless Vertical Handoffs (VHO) between heterogeneous wireless access networks. In general, heterogeneous networks can be combinations of many different kinds, e.g., Vehicular Ad hoc Network (VANET), WLAN, Universal Mobile Telecommunications System (UMTS), CDMA2000 (Code Division Multiple Access), and Mobile Ad hoc Network (MANET). Many new architectures or schemes have been proposed recently for seamless integration of various wireless networks. However, the integration of WLANs and cellular networks has attracted the most attention because currently WLANs and cellular networks coexist and many cellular devices have dual RF interfaces for WLANs and cellular access. With regard to vertical handoff performance, there is a critical need for developing algorithms for connection management and optimal resource allocation for seamless mobility. In this paper, we focus on developing such algorithms based on suitable optimization criteria. Since WLAN and cellular access technologies are commonly available and complementary, we focus on these technologies in this paper but our algorithms are widely applicable across any set of access technologies and applications.

Several interworking mechanisms have been proposed in [1]-[4] to combine WLANs and cellular data networks into integrated wireless data environments. Two main architectures [2]-[4] have been proposed for interworking between 802.11 WLAN and 3G cellular systems: (1) Tight coupling and (2) Loose coupling (see Fig. 1). When the loose coupling scheme is used, the WLAN is deployed as an access network complementary to the 3G cellular network. In this approach, the WLAN bypasses the core cellular networks and data traffic is routed more efficiently to and from the Internet without having to go over the cellular networks which could be a potential bottleneck. However, this approach mandates the provisioning of special Authentication, Authorization, and Accounting (AAA) servers on the cellular operator for interworking with WLANs' AAA services. On the

This research was supported in part by the NIST/Office of Law Enforcement Standards (OLES). It was also supported in part by the Korea Science and Engineering Foundation (KOSEF) grant funded by the Korea government (MOST) (R01-2006-000-10614-0)

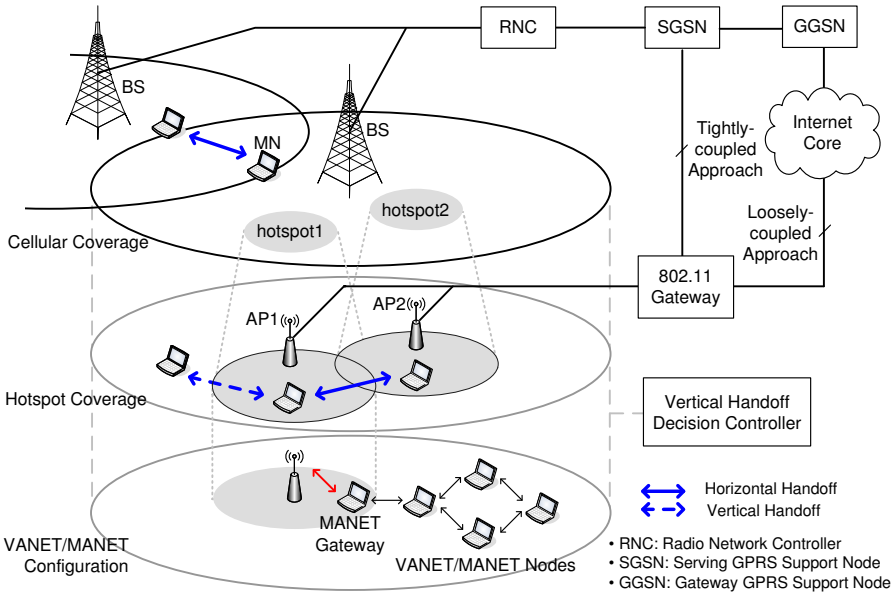


Fig. 1. Architecture of an integrated heterogeneous network consisting of WLAN, cellular and VANET/MANET.

other hand, when the tight coupling scheme is used, the WLAN is connected to the cellular core network in the same manner as any other 3G Radio Access Network (RAN), so that the mechanisms for mobility, QoS and security of the 3G core network such as UMTS can be reused. As a result, a more seamless handoff between cellular and WLAN networks can be expected in the tightly coupled case as compared to the same for the loosely coupled case.

There have also been some research efforts to connect a mobile device equipped with multiple RF interfaces to the most optimal network among a set of available heterogeneous access networks. Vertical mobility is achieved by switching the interface of the mobile device to connect to an alternative target network.

The authors of [6] introduced important performance criteria to evaluate seamless vertical mobility, e.g. network latency, congestion, battery power, service type, etc. In [7], the authors proposed an end-to-end mobility management system that reduces unnecessary handoff and ping-pong effects by using measurements on the conditions of different networks. In [8], various network layer based inter-network handover techniques have been addressed and their performance is evaluated in a realistic heterogeneous network testbed. The authors of [9] propose a vertical handoff decision method that simply estimates the service quality for available networks and selects the network with the best quality. However, there still lie ahead many challenges in integrating cellular networks and WLANs (or any combination of heterogeneous networks in general). As the authors of [5], [6] and [9] have pointed out, known vertical handoff algorithms are not adequate to coordinate the QoS of many individual mobile users or adapt to newly emerging performance requirements for handoff and changing network status. Further, under the current WLAN technology, each mobile device selects an AP for which the Received Signal Strength (RSS) is maximum irrespective of the neighboring network status. Although the attachment to the closest AP is known to consume the least power for the individual mobile device at a given instant, in a situation where many mobile devices try to handoff to the same AP, there would be in effect significantly more power consumption at the mobile devices collectively due to increased congestion delays at the AP. In this paper, we tackle the following problem: given a network of Base Stations (BSs), Access Points (APs) and Mobile Nodes (MNs), and given that an MN is currently experiencing weak or degrading RSS from its current attachment point (BS or AP), how do we find an appropriate attachment point for the MN to connect to (via vertical or horizontal handoff) while optimizing a well defined objective function? Our objective function includes consideration of battery life of MNs and load balancing across attachment points. For seamless integration of WLAN and 3/4G wireless networks, we propose a vertical handoff decision (VHD) algorithm that not only maximizes the overall battery lifetime of MNs in the same coverage area but also seeks to equitably distribute the traffic load across available APs and BSs. We suggest that this proposed algorithm be implemented in multiple vertical handoff decision controllers (VHDC). These VHDCs are

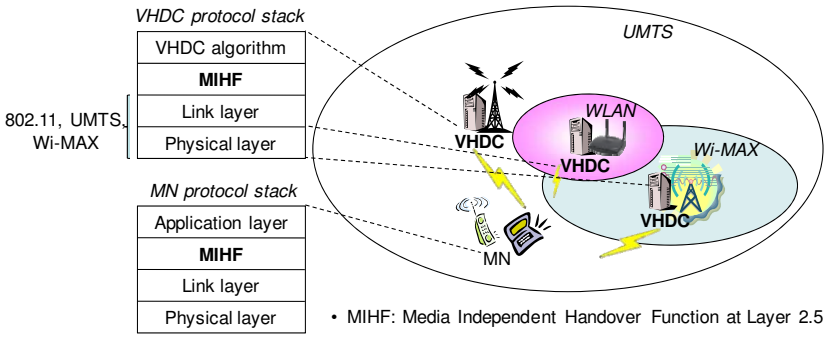


Fig. 2. Illustration of VHDC implementation based on IEEE 802.21 MIHF.

located in the access networks, and can provide the VHD function for a region covering one or multiple APs and/or BSs. We envision that the decision inputs for the VHDCs will be obtainable via the Media Independent Handover Function (MIHF), which is being defined in IEEE 802.21 [10]. Moreover, when ad hoc mode is applied to 3/4G wireless data networks, VANETs and IEEE 802.11 WLANs for more seamless integration of heterogeneous wireless networks (see Fig. 1), we devise a route selection algorithm to forward data packets to the most appropriate AP/BS in order to maximize the same objective function as stated above. Results based on a detailed performance evaluation study are also presented here to demonstrate the efficacy of the proposed algorithms. It may be mentioned here that route selection algorithms have been previously studied in the context of WLAN or cellular networks separately [11][12].

The rest of the paper is organized as follows. We first describe our heterogeneous wireless networking system model and the high-level procedure followed by the VHDC in Section II. Then in Section III, we describe the details of optimization algorithms to select an appropriate attachment point. In Section IV, we present a route selection algorithm in heterogeneous wireless networks that include an ad hoc network (such as VANET or MANET), while taking into account the amount of traffic to be forwarded and the load at attachment points in the route. In Section V, extensive simulation results are presented and the performance of the proposed algorithms is discussed. Finally, the conclusions are stated in Section VI.

## II. Vertical Handoff Decision System Description

As shown in Fig. 2, an MN can be existing at a given time in the coverage area of an UMTS alone. But due to mobility, it can move into the regions covered by more than one access networks, i.e. simultaneously within the coverage areas of, say, an UMTS BS and an 802.11 AP. Multiple 802.11 WLAN coverage areas are usually contained within an UMTS coverage area. A Wi-MAX coverage area can overlap with WLAN and/or UMTS coverage areas. In dense urban areas, even the coverage areas of multiple UMTS BSs can overlap. Thus, at any given time, the choice of an appropriate attachment point (BS or AP) for each MN needs to be made, and with vertical handoff capability the service continuity and QoS experience of the MN can be significantly enhanced. A single operator or multiple operators may operate the BSs and APs within a coverage area. Thus, multiple access technologies as well as multiple operators are typically involved in vertical handoff decisions. Hence, there is a need for a common language in which the link layer information and MNs' battery power information can be exchanged between different networks and/or operators. As described below, this common language is provided by the Media Independent Handover Function (MIHF) of IEEE 802.21.

We also show in Fig. 2 how we envision the Vertical Handoff Decision (VHD) to be implemented. We suggest that our proposed VHD algorithm (described in detail in Section III) be implemented in multiple Vertical Handoff Decision Controllers (VHDC). These VHDCs are located in the access networks as shown in Fig. 2, and can provide the VHD function for a region covering one or multiple APs and/or BSs. We envision that the decision inputs for the VHDCs will be obtainable via the MIHF, which is being defined in IEEE 802.21 [10]. The VHDC is conceptually a network-controlled mobility management entity utilizing the 802.21 MIHF and some experimental implementations of this nature are in progress [13][14]. The MIHF facilitates standards-based message exchanges between the various access networks (or attachment points) to share information about the current link layer conditions, traffic load,

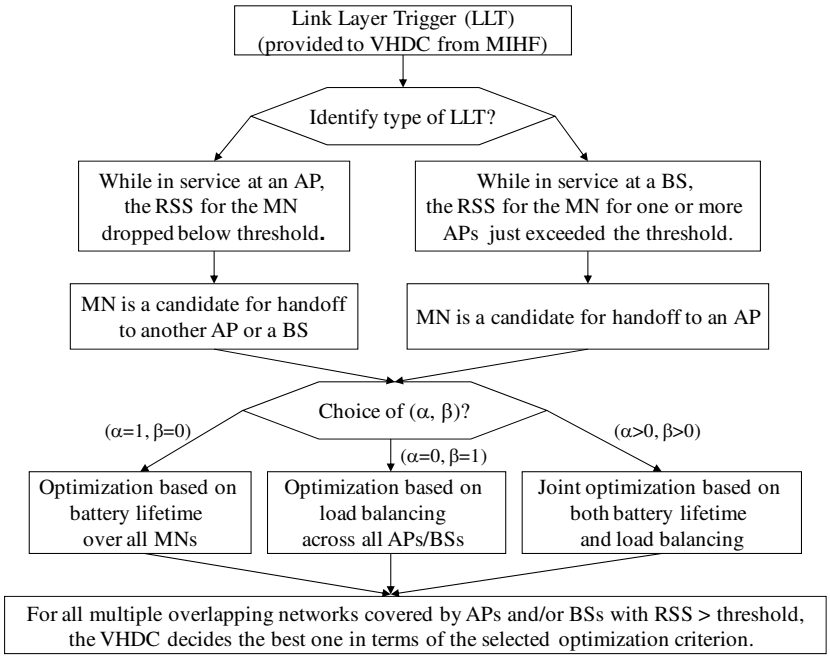


Fig. 3. Flow chart for the high-level procedure used by the VHDC.

network capacities, etc. The MIHF at an access point also maintains the battery life information of the MNs, which are currently serviced by it.

The goal of our proposed VHDC is to facilitate optimization of the overall performance of the integrated system of access networks, specifically, in terms of overall battery lifetime and load balancing. Fig. 3 illustrates the high-level procedure followed by the VHDC for making vertical handoff decisions. The algorithmic and mathematical details of this procedure are described in Section III. As shown in Fig. 3, the VHDC obtains Link Layer Triggers (LLTs) via MIHF [15][16]. An LLT regarding an MN typically indicates one of these two possibilities: (a) While in service at an AP, the RSS for the MN has dropped below a specified threshold, or (b) While in service at a BS, the RSS from one or more APs has just exceeded a specified threshold. In general, if an MN's connection can be supported by an available BS as well as an available AP, then the AP would be the preferred attachment point for that MN. This is due to the higher data rate as well as lower bandwidth cost associated with an AP as compared to that for a BS. If the LLT indicates possibility (a), then the VHDC tries to search for other networks for connection handoff. In the case that there exist multiple choices of APs for handoff, the VHDC evaluates the APs and then directs a handoff operation to the network with optimal performance/cost. On the other hand, if no other APs are found for a possible handoff, then the cellular network would be then considered the best available wireless network. If the LLT indicates possibility (b), then the MN would be a candidate for vertical handoff from a BS (UMTS or Wi-MAX) to an AP (WLAN). As described before, the performance/cost can be in the form of the collective battery lifetime of the MNs and/or load balancing across the APs/BSs. We can choose a performance metric that is tunable with weighing parameters, $\alpha$ and $\beta$, and could be tuned to represent only longevity of battery lifetime over all MNs or only load balancing across all APs/BSs, or a weighted combination of the two. As seen at the last step in the procedure of Fig. 3, irrespective of current network type, the VHDC decides the best one amongst multiple overlapping networks (covered by APs or BSs), based on a selected optimization criterion. The details of this last step follow in the next section.

## III. Vertical Handover Decision Algorithm to Optimize the System Performance

In this section, details of the optimization techniques used in our vertical handoff decision algorithm and implemented in the VHDC are provided. The WLAN hotspots are typically configured as small cells within the aforementioned "cellular coverage area" of GPRS/UMTS or CDMA2000 which is relatively larger compared with WLAN hotspots as shown in Fig. 1. Since many variables are used in this paper, a glossary of variable names and definitions is provided in Table I.

Let $A = \{a_1, \cdots, a_N\}$ and $C = \{c_1, \cdots, c_M\}$ be the sets of APs in a cellular coverage area and BSs covering the cellular coverage area, respectively. Note

TABLE I
GLOSSARY OF VARIABLE DEFINITIONS

| Variable | Definition |
|---|---|
| $N$ | Number of APs |
| $M$ | Number of BSs |
| $\bar{U}$ | Set of all Mobile Node (MNs) |
| $\|\bar{U}\|$ | Total number of MNs ($K$) |
| $u_j$ | MN $j$ ($1 \le j \le K$) |
| $r_j$ | Bandwidth (i.e., data rate) requested by $u_j$ ($1 \le j \le K$) |
| $U_t$ | Set of MNs requesting vertical handoff (VHO) at time $t$ |
| $\|U_t\|$ | Number of MNs requesting handoff at time $t$ (equals $m(t)$) |
| $V_t$ | $V_t = \bar{U} - U_t$ |
| $V_t^{(a)}$ | Subset of MNs in $V_t$ that have connection in a WLAN at $t$ |
| $V_t^{(c)}$ | Subset of MNs in $V_t$ that have connection in a cellular network at $t$ |
| | $V_t = V_t^{(a)} + V_t^{(c)}$ or $V = V_a + V_c$ (dropping $t$) |
| | $U_t, V_t, V_t^{(a)}, V_t^{(c)} \Rightarrow U, V, V_a, V_c$ (dropping $t$) |
| $\|V_a\|$ | Number of MNs that have a connection in a WLAN at time $t$ |
| $\|V_c\|$ | Number of MNs that have a connection in a a cellular network at time $t$ |
| $\hat{i}$ | $i - N$; $1 \le \hat{i} \le M$ corresponds to $N+1 \le i \le N+M$ |
| $B_i$ | Maximum bandwidth which an AP $a_i$ ($1 \le i \le N$) can provide |
| $B_{\hat{i}}^{(c)}$ | Maximum bandwidth which a BS $c_{\hat{i}}$ can provide |
| $w(i)$ | Price/weight for WLAN and cellular bandiwdths; $w_a$ ($1 \le i \le N$) and $w_c$ ($N+1 \le i \le N+M$) |
| $e_{ij}$ | Effective bandwidth of MN $u_j$ when it is attached to AP $i$ |
| $e_{ij}^{(c)}$ | Effective bandwidth of MN $u_j$ when it is attached to BS $i$ |
| $\rho_i$ | Load at AP $a_i$ ($1 \le i \le N$); Load at BS $c_i$ ($N+1 \le i \le N+M$) |
| $z_i$ | Equals $B_i$ for $0 \le i \le N$ and $B_{\hat{i}}^{(c)}$ for $N+1 \le i \le N+M$ |
| $p_j$ | Available battery power of MN $j$ |
| $p_{ij}$ | Power consumption rate per unit time for MN $j$ when attached to AP $a_i$ |
| $p_{ij}^{(c)}$ | Power consumption rate per unit time for MN $j$ when attached to BS $c_i$ |
| $p_j^b$ | Power consumption amount per byte of transmission at MN $j$ |
| $RSS_{ij}$ | Received signal strength for MN $j$ from AP $a_i$ or BS $c_i$ |
| $\theta_a$ | RSS threshold to connect to AP |
| $\theta_c$ | RSS threshold to connect to BS |

that usually $M = 1$ except in the case of a highly dense urban deployment. Even when $M > 1$, $M$ is much smaller than $N$ because typically many APs are deployed within a cellular coverage area. The VHDC maintains the sets $A$ and $C$ covering the cellular coverage area as a list of candidate attachment points. It adds all available WLAN access points (APs) into the set $A$, and collects the information about load status on every AP in the set $A$ and every BS in the set $C$. Note that in this section, we take into account only $a_i \in A$ $(1 \le i \le N)$ and $c_{\hat{i}} \in C$ $(1 \le \hat{i} \le M)$ as candidate attachment points, whereas in the next section, each Mobile Node (MN) in ad hoc networking mode would also be considered as a possible attachment point. In the cellular coverage area, $\bar{U} = \{u_1, \cdots, u_K\}$ is defined as the set of all MNs. Each MN is either requesting a handoff (or just turned on) or currently serviced by an AP ($\in A$) or BS ($\in C$) with no need for mobility at the time of optimization decision. Thus, the set $\bar{U}$ can be divided into the following two subsets at certain time $t$:

$$U_t = \{u_{n_1}, u_{n_2}, \cdots, u_{n_{m(t)}}\}$$

where $m(t)$ is the number of MNs requesting handoff at time $t$ and $n_1, ..., n_{m(t)}$ are the corresponding indexes of those MNs, and

$$V_t = \bar{U} - U_t$$

which represents the set of MNs that have a good connection (i.e., not requiring handoff) to an AP or a BS.

Each AP $a_i$ and BS $c_{\hat{i}}$ are assumed to have a maximum bandwidth, $B_i$ and $B_{\hat{i}}^{(c)}$, respectively. Let $\hat{i}$ denote $i-N$ ($N+1 \le i \le N+M$). Let $w(i)$ ($1 \le i \le N+M$) denote the predefined costs or weights for the bandwidths of AP $a_i$ ($1 \le i \le N$) and BS $c_{\hat{i}}$ ($N+1 \le i \le N+M$). For simplicity, we define two different weights depending on whether the wireless access network is WLAN or cellular network. That is, for APs $a_i \in A$ ($1 \le i \le N$), $w(i) = w_a$, and $w(i) = w_c$ for BSs $c_{\hat{i}}$ ($1 \le \hat{i} \le M$). Each $a_i \in A$ has a limited transmission range and serves only users that reside in its range. The set $V_t$ is divided into subsets $V_t^{(a)}$ and $V_t^{(c)}$ depending on whether $u_j \in V_t$ has a connection in a WLAN or a cellular network, respectively. Note that the $|U_t|$ MNs that are candidates

for vertical handoff can belong in a WLAN or a cellular network, subsequent to the handoff decision.

For 802.11 products, it is known that an AP is able to maintain the average bit rate information for the MNs which are currently associated with it [17][18]. Thus, each AP ($a_i \in A$) or BS ($c_{\hat{i}} \in C$) can maintain the effective data rate, $e_{ij}$ and $e_{\hat{i}j}^{(c)}$ for MN $u_j$ when it belongs to $V_t^{(a)}$ or $V_t^{(c)}$, respectively. However, for each MN $u_j \in U_t$, the AP to which the MN will handoff is not able to evaluate the effective data rate for the MN due to the absence of active signaling between the AP and the MN when they are not connected. Thus, a requested data rate, $r_j$ is defined for each MN $u_j \in U_t$. Otherwise, if we assume that every MN is equipped with client software that periodically collects the bit rate information for every AP/BS in its neighborhood by using beacon messages/pilot bursts, it is possible to evaluate the effective bit rate, $e_{ij}$ and $e_{\hat{i}j}^{(c)}$ from each AP $a_i \in A$ and BS $c_{\hat{i}} \in C$, respectively, to each MN $u_j \in U_t$. The collected information about the effective bit rate is available to the VHDC via the 802.21 MIHF.

Since our proposed selection algorithms are performed at a certain time instant $t$, from now on, we shall omit the subscript $t$ from $U_t$, $V_t$, $V_t^{(a)}$, and $V_t^{(c)}$ for notational convenience and for the clarity of understanding. Thus, $U$, $V$, $V_a$, and $V_c$ will be used instead. Now, we define the load, $\rho_i$, on AP $a_i$ or on BS $c_{\hat{i}}$ in a cellular coverage area as follows:

DEFINITION 1 *For each AP $a_i \in A$ ($1 \le i \le N$), the load on AP $a_i$ is*

$$\rho_i = \sum_{u_j \in V_a} e_{ij}, \quad \textit{for } 1 \le i \le N \tag{1}$$

*while the load on BS $c_{\hat{i}}$ is*

$$\rho_i = \sum_{u_j \in V_c} e_{\hat{i}j}^{(c)}, \quad \textit{for } N+1 \le i \le N+M. \tag{2}$$

The above definition of load deliberately does not take into account the calls that are requesting handoff and will move away from the AP in consideration at the time decision is made. As a matter of fact, it is possible to compute $\rho_i$ ($1 \le i \le N+M$) because an AP or BS is able to maintain the bit rate information for all the MNs connected to itself.

Associated with each MN $u_j$ ($1 \le j \le K$) is a quantity $p_j$, denoting the available amount of power or the initial amount of power when it is just attached to a network. Normally, $p_j$ would be at its maximum when the battery is fully charged. Let $p_{ij}$ denote the power consumption per unit of time needed at MN $u_j$ ($1 \le j \le K$) to reach an AP $a_i$ ($1 \le i \le N$). The value of $p_{ij}$ depends on the number of MNs attached to AP $a_i$ and the data rate requested by MN $u_j$. That is, the larger the number of power-on nodes attached to the same AP, the more power is consumed by each MN because they each get lower rate and hence need to connect longer. With greater use of applications requiring higher data rate, the MN will consume power at higher rates. Thus, the amount of load at AP has an impact on the power consumed by MNs as $p_{ij} \propto \rho_i$. Similarly, $p_{\hat{i}j}^{(c)}$ ($\propto \rho_{N+\hat{i}}$) stands for the power level needed at MN $u_j$ to reach BS $c_{\hat{i}}$.

When each MN $u_j$ ($1 \le j \le K$) is associated with a certain AP $a_i$ ($1 \le i \le N$) or BS $c_{\hat{i}}$ ($1 \le \hat{i} \le M$), a formal definition of battery lifetime matrix for MNs with respect to each attachment point in the cellular coverage area is given as follows:

DEFINITION 2 *Let $\mathbf{L} = \{l_{ij}\}_{(N+M)\times K}$ be the battery lifetime matrix where the matrix element, $l_{ij}$ ($1 \le i \le N+M$) denotes the battery lifetime of $u_j$ supposing that MN $u_j$ hands off to AP $a_i$ ($1 \le i \le N$) while $l_{(N+\hat{i})j}$ ($1 \le \hat{i} \le M$) is the battery lifetime of $u_j$ in case that MN $u_j$ hands off to BS $c_{\hat{i}}$. Then, for each MN $u_j$ ($1 \le j \le K$), we have*

$$l_{ij} = \frac{p_j}{p_{ij}}, \qquad \textit{for } 1 \le i \le N \tag{3}$$

*and*

$$l_{ij} = \frac{p_j}{p_{\hat{i}j}^{(c)}}, \qquad \textit{for } N+1 \le i \le N+M. \tag{4}$$

*where it is assumed that every $l_{ij} > 0$ in this study.*

The significance of the assumption that $l_{ij} > 0$ is that the MNs never disconnect due to battery outage. Thus, the population of MNs in the system remains constant. In our simulation tests, this is ensured by choosing a sufficient large initial battery power for all MNs. The matrix $\mathbf{L}$ plays a significant role in decisions at the VHDC regarding which attachment point should be selected among the sets $A$ and $C$ for the MNs requiring handoff. The different cost functions used in the optimization methods leading to handoff decisions will be defined formally later in this section.

To formulate the optimal vertical handoff decision problem, a binary variable $x_{ij}$ is defined to have a value one ($x_{ij} = 1$) if user $u_j$ is associated with AP $a_i$ ($1 \le i \le N$) or BS $c_{\hat{i}}$ ($N+1 \le i \le N+M$) and zero ($x_{ij} = 0$) otherwise. Let $RSS_{ij}$ ($1 \le i \le N+M$) be Received Signal Strength (RSS) for MN $j$ from AP $a_i$ or BS $c_{\hat{i}}$. Let $\theta_a$ and $\theta_c$ denote RSS thresholds for MN's connection to AP and BS, respectively. Then, we

can define an association matrix $\mathbf{X}$ consisting of $x_{ij}$ as follows:

DEFINITION 3 *Let $\mathbf{X} = \{x_{ij}\}_{(N+M)\times K}$ be an association matrix for a cellular coverage area such that*

$$\sum_{1\le i\le N+M} x_{ij} = 1, \qquad \textit{for } 1 \le j \le K \tag{5}$$

$$x_{ij} \in \{0, 1\} \tag{6}$$

*and*

$$x_{ij} = 0 \textit{ if } RSS_{ij} < \begin{cases} \theta_a & \textit{for } 1 \le i \le N \\ \theta_c & \textit{for } N+1 \le i \le N+M \end{cases} \tag{7}$$

*where $x_{ij}$ ($1 \le i \le N$, $1 \le j \le K$) and $x_{(N+\hat{i})j}$ ($1 \le \hat{i} \le M$, $1 \le j \le K$) are binary indicators, each of which has a value of 1 if and only if, for the former, MN $u_j$ hands off to AP $a_i$ while for the latter, MN $u_j$ hands off to BS $c_{\hat{i}}$. Moreover, let $\mathcal{X}$ be the set of all association matrices.*

The BSs collectively provide full coverage for the entire region of interest. The above DEFINITION 3 accordingly assures that each MN requesting handoff is covered by either a BS or an AP.

DEFINITION 4 *The battery lifetime of MN $u_j \in U$ for an association matrix $\mathbf{X} = \{x_{ij}\}$, $lt_j(\mathbf{X})$ is defined as*

$$lt_j(\mathbf{X}) = \sum_{1\le i\le N+M} l_{ij}x_{ij} \tag{8}$$

We can define the requested data rate on AP $a_i$, and on BS $c_{\hat{i}}$ for an arbitrary association matrix as follows:

DEFINITION 5 *Let $\gamma_i$ ($1 \le i \le N+M$) denote total requested data rate on AP $a_i$ ($1 \le i \le N$) and BS $c_{\hat{i}}$ ($1 \le \hat{i} \le M$). Let $r_j$ denote the data rate requested by MN $u_j$ ($1 \le j \le K$). Then, for any $\mathbf{X} = \{x_{ij}\} \in \mathcal{X}$,*

$$\gamma_i(\mathbf{X}) = \sum_{u_j\in U} r_j x_{ij} \tag{9}$$

In case each MN $u_j \in U$ is able to evaluate the effective bit rate $e_{ij}$ and $e^{(c)}_{\hat{i}j}$ from the candidate APs (i.e., those with $RSS_{ij} > \theta_a$) and the candidate BSs (i.e., those with $RSS_{ij} > \theta_c$), Eq. (9) in DEFINITION 5 is replaced by

$$\gamma_i(\mathbf{X}) = \begin{cases} \sum_{u_j\in U} e_{ij}x_{ij} & \text{for } 1 \le i \le N \\ \sum_{u_j\in U} e^{(c)}_{\hat{i}j}x_{ij} & \text{for } N+1 \le i \le N+M. \end{cases} \tag{10}$$

For the given battery lifetime matrix $\mathbf{L}$, we formulate the vertical handoff decision problem to maximize the battery lifetime (network wide) as follows:

$$\textbf{Max-}L : \text{Max}_{\forall \mathbf{X}\in\mathcal{X}} \sum_{u_j\in U} lt_j(\mathbf{X}) \tag{11}$$

subject to

$$\rho_i + \gamma_i(\mathbf{X}) \le \begin{cases} B_i, & \text{for } 1 \le i \le N \\ B^{(c)}_{\hat{i}}, & \text{for } N+1 \le i \le N+M \end{cases} \tag{12}$$

where the constraint in Eq. (12) ensures that the total load on each attachment point cannot exceed the maximum bandwidth supported by each AP or BS. With regard to Eq. (11), it may be noted that the battery lifetimes of $u_j \in V$, where $V = V_a \cup V_c$, do not play a role in optimization (at each decision epoch). However, all MNs are included for reporting the average remaining battery lifetime in the course of our simulations (Section V).

In the problem formulation of **Max-**$L$ in Eq. (11), the total battery lifetime of the system is maximized without considering fairness with regard to individual battery lifetime of different MNs. Thus the max-min fairness is taken account of as follows:

$$\textbf{Max/Min-}L : \text{Max}_{\forall \mathbf{X}\in\mathcal{X}} \left( \text{Min}_{1\le j\le K} lt_j(\mathbf{X}) \right) \tag{13}$$

subject to the same constraint as stated for **Max-**$L$ in Eq. (12). While the earlier formulation of **Max-**$L$ in Eq. (11) increases the total battery lifetime, it may in some situations compromise MNs with already lower remaining power. So we mention this alternative **Max/Min-L** formulation, but in this paper our focus is more towards joint optimization of battery lifetime and fairness in terms of distributedness of load at APs/BSs.

We now turn to the problem of distributing the overall load in a cellular coverage area. LEMMA 1 in the Appendix A captures the fact that minimizing the sum of squared numbers is equivalent to minimizing the standard deviation of the numbers when the mean is constant. Since the standard deviation represents the degree of variation, we aim for the load per AP or BS in the cellular coverage area to stabilize around a mean value $M$ with small deviations.

PROPERTY 1 *The total load from all MNs of $U$, $\sum_{1\le i\le N+M} \gamma_i(\mathbf{X})$, does not change irrespective of what values $\mathbf{X}$ has. Thus, in a cellular coverage area, the expression $\frac{1}{N+M}\sum_{1\le i\le N+M} w(i)\Big(\frac{\rho_i+\gamma_i(\mathbf{X})}{z_i}\Big)$ also becomes invariant to the decision (i.e., $\mathbf{X}$) at the time of performing the optimization algorithm, where $z_i$ is a maximal load which each AP or BS can tolerate.*

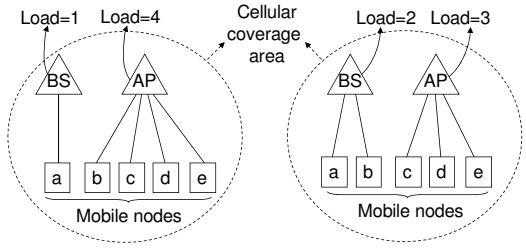


(a) Case 1 (b) Case 2

Fig. 4. Examples of achieved load distribution across attachment points when **Opt-**$F$ is applied.

In the above PROPERTY 1, $z_i = B_i$ for $1 \le i \le N$ and/or $z_i = B_{\hat{i}}^{(c)}$ for $N+1 \le i \le N+M$ (as in Eq. (12)), noting that $\hat{i} = i - N$.

On the basis of LEMMA 1 (in Appendix A) and PROPERTY 1, we define a load-based cost function, $F$, and formulate the following optimization for distributedness of load:

$$\textbf{Opt-}F : \text{Min } F = \text{Min}_{\forall \mathbf{X} \in \mathcal{X}} \sum_{1 \le i \le N+M} w(i) \Big( \frac{\rho_i + \gamma_i(\mathbf{X})}{z_i} \Big)^p \tag{14}$$

subject to

$$\rho_i + \gamma_i(\mathbf{X}) \le z_i, \qquad \text{for } 1 \le i \le N+M \tag{15}$$

where $p = 2$ is recommended (see discussion below). Minimizing the cost function in Eq. (14) results in preventing BSs and APs with already higher load from being more congested.

Figs. 4-(a) and 4-(b) illustrate and compare two cases of the achieved load distributions using Eq. (14). In this example, $K = 5$, $M = 1$, and $N = 1$. Consider a cellular coverage area with two attachment points and 5 mobile users named from 'a' to 'e', where it is assumed that the weights of each MN for cellular network and WLAN are the same (i.e., $w_c = w_a$) and the maximum available bandwidth at an AP or a BS is 5 (i.e., $z_1 = z_2 = 5$) for simplicity. Assume that the data rate to every MN is 1. When $p = 1$, the attachment point selection may result in Fig. 4-(a) or Fig. 4-(b) because $\frac{1}{5} + \frac{4}{5} (= 1) = \frac{2}{5} + \frac{3}{5} (= 1)$. That is, when $p = 1$, there is no difference between the two cases in Figs. 4-(a) and 4-(b) because the total load in the two cases is the same. However, when $p = 2$, the attachment points are selected as in Fig. 4-(b) because $(\frac{1}{5})^2 + (\frac{4}{5})^2 (= 0.68) > (\frac{2}{5})^2 + (\frac{3}{5})^2 (= 0.52)$ on the basis of Eq. (14).

Thus, the cost function in Eq. (14) with $p = 2$ provides fairness from load balancing point of view when deciding an attachment point for an MN that requires handoff. Due to the fact that the wireless users associated with an AP share the buffer and bandwidth at the AP, the consideration of fairness works towards mitigating user congestion at APs.

In order to accomplish a joint optimization of the total battery lifetime and the fairness of load in a cellular coverage area, we formulate a combined cost function with parameters $\alpha$ and $\beta$ as follows:

$$G(\mathbf{X}, \alpha, \beta) = \alpha \sum_{u_j \in U} lt_j(\mathbf{X}) - \beta \sum_{1 \le i \le N+M} w(i) \Big( \frac{\rho_i + \gamma_i(\mathbf{X})}{z_i} \Big)^2 \tag{16}$$

Minimizing the cost function in Eq. (14) is equivalent to maximizing the negative of the same cost function because $\frac{\rho_i + \gamma_i(\mathbf{X})}{z_i} < 1$. Thus, we have the joint optimization statement of the total battery lifetime and the fairness of the load as follows:

$$\textbf{Opt-}G : \text{Max } G(\mathbf{X}, \alpha, \beta) \tag{17}$$

with the constraints of Eq. (15). In Eq. (17), when $\alpha = 1$ and $\beta = 0$, it is evident that the Eq. (17) is an equivalent optimization problem of Eq. (11). Further, the optimization problem, $\text{Max}_{\forall \mathbf{X} \in \mathcal{X}} G(\mathbf{X}, 0, 1)$ subjected to the constraint in Eq. (15), is equivalent to **Opt-**$F$.

## IV. OPTIMIZATION OF BATTERY LIFETIME IN HETEROGENEOUS NETWORKS INCLUDING AD HOC MODE

### *A. Integrated WLAN and Cellular Networking System Including Ad Hoc Networking Mode*

Now we consider network architectures where, in addition to cellular networks and WLANs, peer-to-peer communications is further enabled using the IEEE 802.11 ad hoc mode [11]-[12] (also see Fig. 1). Now see seek to generalize the algorithm to select the most appropriate attachment point by considering the further selection of intermediate MNs to relay data packets to that attachment point.

In this system with ad hoc networking, cooperating MNs form a MANET/VANET using the IEEE 802.11 interface in an ad hoc mode. When an MN which is actively receiving data frames from a BS of cellular network or an AP, experiences low downlink channel rate and the VHDC cannot find an alternative direct attachment point (i.e., BS or AP) for the MN, a route will be selected via the MANET/VANET to allow the MN to access an appropriate attachment point.

The Dynamic Source Routing (DSR) technique [19][20] is used with suitable modification as the underlying route discovery protocol in our system. As shown in Fig. 5, the MN (i.e., source labeled as *src*) sends out a *route request* message using its IEEE 802.11 interface. This *route request* message is broadcast through the ad

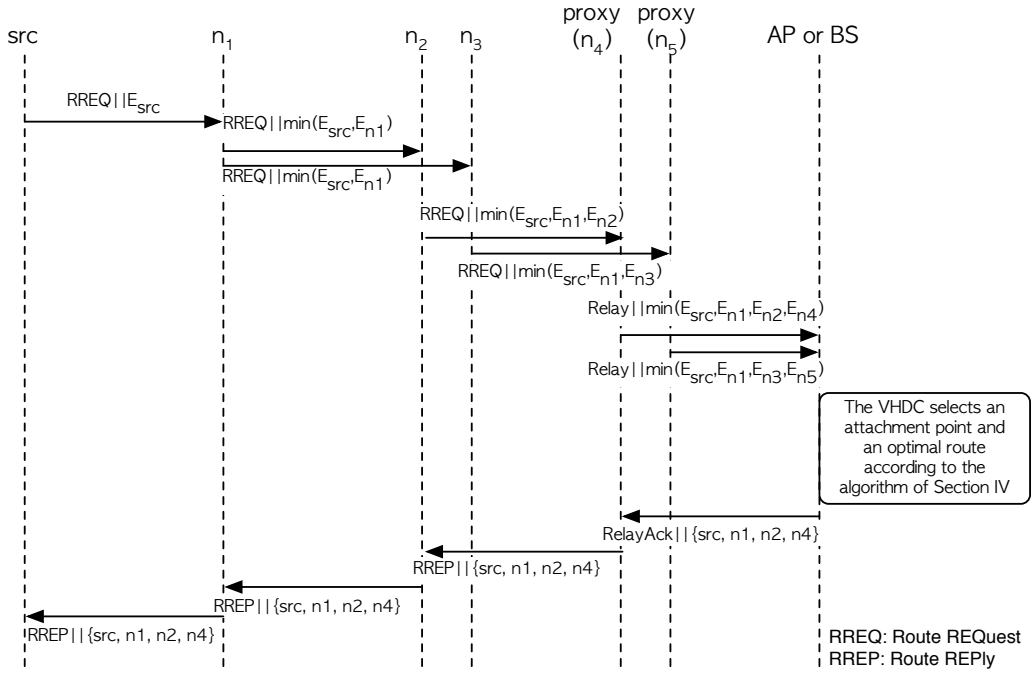


Fig. 5. Example procedure to discover a relay route to a proxy node, where a relay route {source, node $n_1$, node $n_2$, proxy node $n_4$} is selected.

hoc network according to the route discovery protocol. The objective is to find an optimal relay route in terms of overall battery lifetime, to reach a node (i.e., proxy node) with high downlink channel rate to an attachment point. In order to prevent the *route request* message from being sent to all APs and the BS in a cellular coverage area, the number of hops is limited by using the Time-to-Live (TTL) field in the *route request*. Thus, the spread of a *route request* is controlled only to nearby attachment points located within pre-designated number of hops over the ad hoc network.

Again referring to Fig. 5, the candidate proxy node sends a *relay* message to its BS or AP. Once the BS or AP receives the *relay* message, the VHDC (in Section II) selects an attachment point and the best route to the attachment point based on the algorithm that is presented in Section IV-B. The selected attachment point updates its routing table entry for the MN while sending a *relay ack* message to the proxy node. Then the proxy node returns a *route reply* to the MN that initiated the *route request*. When the proxy node receives a data frame from the BS or AP, it forwards the frame to the next relay node. This forwarding process continues via the IEEE 802.11 interfaces of all the relay nodes on the selected route till the MN receives the frame. For the case when the downlink channel rate of the proxy node goes below a certain level due to its mobility, DSR is modified for the proxy node to piggyback its degraded downlink channel rate in data frames that are forwarded to the source MN so that it could begin another round of route discovery to find another optimal relay route.

We will now proceed to present the details of the algorithm for selection of the relay and proxy nodes that constitute the source MN's route toward a BS or an AP. This is the algorithm that the VHDC in Fig. 5 implements for selection of the best route in response to the *relay* messages received from the candidate proxy nodes.

### *B. Route Selection Algorithm to Optimize Battery Lifetime of System Including Ad Hoc Mode*

For heterogeneous wireless networks, which include ad hoc networking, we aim to evenly balance over all MNs the battery power consumed in relaying traffic for others. As presented in Section III, in a heterogeneous wireless network without ad hoc support, the battery lifetime of each MN is considered to be related only to the RSS and the congestion (i.e., load) at its attachment point. However, in a heterogeneous wireless network supporting ad hoc mode, the amount of traffic each MN relays has a great impact on the MN's battery lifetime, and hence all MNs in the network must participate fairly in relaying each other's data frames. Thus, in this section, taking account of the amount of traffic load to be forwarded, we develop a route selection algorithm

that maximizes, over the available routes, the remaining battery life of "bottleneck" node which has the lowest residual energy. This results in maximizing the overall battery lifetime of the system as well.

We consider a finite population of $K$ MNs in a cellular coverage area as in Section III. Let $D$ be the amount of traffic in bytes that has to be routed via some MNs in the cellular coverage area. For MN $u_j \in U$ which experiences low downlink channel rate while receiving data frames from a BS of cellular network or an AP, unless the VHDC can find an alternative point-to-point (one-hop) attachment point, a route will be selected by using ad hoc networking. Thus, the data from MN $u_j$ is relayed over other MNs in the ad hoc network in order to reach an appropriate attachment point. Let $p_j^b$ be the power consumption amount per byte of transmission at a given MN $u_j$. Then, the cost function is defined as:

$$E_j = \frac{p_j}{p_j^b D}. \tag{18}$$

The maximum battery lifetime resulting from selection of a given route, $r_s$, is determined by the minimum value of $E_j$ over the path, that is:

$$L_s = \text{Min}_{\forall u_j \in r_s} E_j. \tag{19}$$

Let $R$ be the set of all possible routes between the MN $u_j$ that is experiencing degraded downlink channel rate and candidate attachment points via proxy MNs in the ad hoc network. We assume that the VHDC has already selected (using **Opt-**$G$ in Eq. (17)) the optimal attachment point (AP or BS) with which the candidate proxy node is associated. Then, we select the route $r_{max}$ with the maximum battery lifetime value from the set $R$ as follows:

$$\begin{aligned} r_{max} : \ & \text{Max}_{\forall r_s \in R} L_s \\ & = \text{Max}_{\forall r_s \in R} \Big( \ \text{Min}_{\forall u_j \in r_s} \ \frac{p_j}{p_j^b D} \ \Big) \end{aligned} \tag{20}$$

When the route discovery process is triggered for an MN $u_j$ that is experiencing low downlink channel rate, the battery lifetime information i.e. $E_j$, is sent encapsulated in the header of a *route request* message as a *cost* field. When a relay node $u_i$ ($i \neq j$) receives the *route request* message, it calculates the value of $E_i$ and compares it with the *cost* field in the received *route request*. If the calculated $E_i$ is less than the value of the *cost* field, then $E_i$ is copied into the *cost* field. This process is repeated until the *route request* message reaches a BS or an AP which has been selected by the VHDC using **Opt-**$G$. The sequence of signal flows corresponding to their operations are shown in Fig. 5.

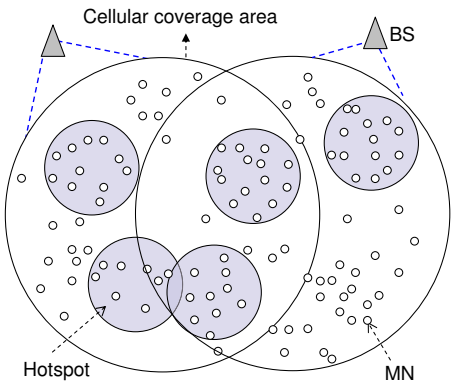


(a) Two cases of 50 and 100 MNs for 2 BSs and 5 APs

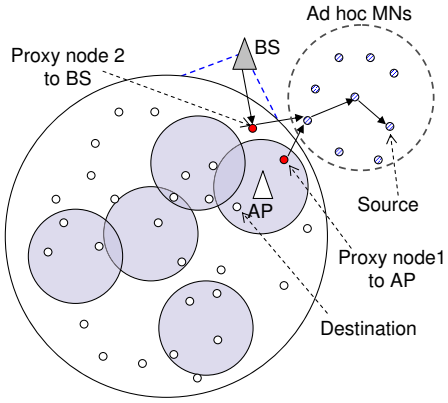


(b) Network topology with ad hoc mode

Fig. 6. Simulation topologies of heterogeneous wireless networks.

## V. Performance Evaluation

Eqs. (11), (14) and (17) in Section III are Mixed Integer Programming (MIP) formulations for battery lifetime maximization and load balancing. These MIP problems can be solved using the well known branch and bound algorithm [21]. First, we describe the simulation setup. Then we present the simulation results detailing the total battery lifetime over all MNs and the load distribution across all APs and BSs.

### A. Simulation Environment

We conducted simulations for a cellular coverage area that is covered by two overlapping BSs and five hotspots as shown in Fig. 6-(a). Further, Fig. 6-(b) shows our simulation topology for the case when MANET/VANET is used as an enhancement to the cellular network and the hotspots. We simulated two test scenarios in which 50 and 100 MNs are dispersed, respectively, over the combined coverage area of the two BSs in the topology of Fig. 6-(a). Within the cellular coverage area, each hotspot area is conceptually divided into three different concentric areas as shown in Fig. 7. The innermost

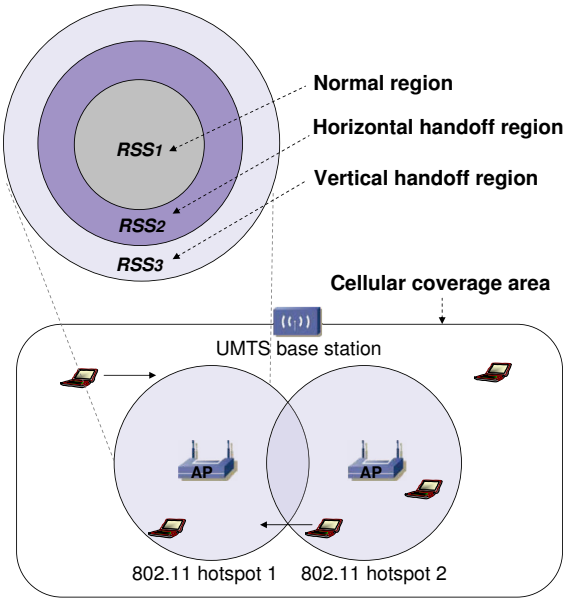


Fig. 7. A conceptual look at RSS in a WLAN and example handoff regions in a heterogeneous network

area, $RSS_1$, has the strongest RSS while the second area, $RSS_2$, which is outside $RSS_1$, has lower RSS than $RSS_1$. And the third area, $RSS_3$, representing the remaining portion of the hotspot area has the weakest RSS. As depicted in Fig. 7, $RSS_2$ region is potentially the horizontal handoff region, whereas $RSS_3$ is potentially the vertical handoff area. It should be noted that in realistic WLAN environments, RSS is highly variable over time even at a fixed location, depending on several known/unknown parameters such as multipath fading, interference, local movements, etc. Instead, for each combination of MN and AP, in order to also factor in multipath fading and other physical layer effects, we select a randomized average RSS value, $RSS_{ij}$, where $i$ and $j$ denote the AP and the MN, respectively. This randomized average RSS value selection is done such that it broadly captures the effects of distance to the AP (e.g., the concentric regions of Fig. 7) and also the effects of the physical layer phenomena and time-averaging.

At the beginning of the simulation run, MNs are evenly distributed over all WLAN areas, and hence 10 MNs (first test case) or 20 MNs (second test case) are serviced by each of the five APs. The MNs move around during the entire simulation time. A random mobility model is used to characterize the movement of MNs inside a cellular coverage area. The $RSS_{ij}$ values for all pairs of MN and AP association are reselected after each such movement, according to the method described above. For simplicity, it is assumed in the simulations that each MN's RSS value is above the required threshold for making a connection to a BS if it is within the coverage area of that BS.

The requested data rate of MN $j$, denoted by $r_j$, can be one of the values from the set {64 kbps, 128 kbps, 192 kbps}. When a new connection arrives, the associated data rate is uniformly selected from the three allowed data rates. The battery power of an MN $j$, denoted by $p_j$, is initialized at the onset of its connection to the value of $10^3$ Joules (J). The rates of consumption of MN $j$'s battery power in association with AP $i$ and with BS $i$ are $p_{ij}$ and $p_{ij}^{(c)}$, respectively. Each of these rates is assumed to be exponentially distributed with a mean of 5 mJ/s [24]. The bandwidth capacities of each AP and each BS, $B_i$ and $B_i^{(c)}$ are set to 20 Mbps and 2 Mbps, respectively. We set the weights (or prices) associated with AP and BS bandwidth usage, $w_a$ and $w_c$, to values 1 and 10, respectively.

In our experiment, we used the TOMLAB[1] optimization package [22] and from the libraries thereof, CPLEX was used to solve the problem formulations described in Section III. We use the branch-and-bound algorithm in the CPLEX optimization package for solving the MIP optimization problems. We studied the battery lifetime and the evenness of load distribution for the two test cases. Ten independent simulation runs of duration 10,000s each were performed, measurements were taken at intervals of 1000s, and the results reported were averaged over the ten runs. Our two key performance metrics were measured over the simulation time considering all MNs, APs, and BSs involved in the two test cases.

It is worth noting here that the computational complexity of the proposed optimization algorithm is very manageable. Also, the computational complexity is limited due to the sparse nature of the $\mathcal{X}$ and $\mathbf{X}$ matrixes (see Eqs. (5) and (7)). Majority of entries in these matrices are zero while performing the optimization computations; only the neighboring networks that have RSS greater than a threshold are relevant from the perspective of MNs that require vertical handoff. All experiments were run on an otherwise unloaded 2 GHz Pentium IV processor with 768MB of memory. On average, the CPU run time taken to solve the optimization was around 10 ms for both the 50-node and 100-node topologies. It is to be noted that these CPU run times are small enough not to be of concern for the optimization computations for VHO network selection in a realistic heterogeneous wireless network. Besides, these measurements were in fact obtained on a simple desktop computer, whereas the

[1]TOMLAB and CPLEX are commercially available software tools. This work makes use of them for generating illustrative simulation results, but NIST does not in any way recommend or favor their use over other similar or comparable products.

VHDC in real implementation would have the benefit of faster processors.

### *B. Simulation Results*

In this section, we present and discuss simulation results for the topology of Fig. 6-(a) and two test cases (50 MNs and 100 MNs) described in Section V-A. To the best of our knowledge, there is no previous proposal that considered similar optimization objectives as we do (namely, maximizing collective battery-life time and load balancing) for heterogeneous networks. Hence, we chose to compare the performance of our methods with that of a commonly known method, namely, the Strongest-Signal First (SSF) method. The SSF method is basically a WLAN-first scheme (i.e., preferring an available WLAN over a cellular network), and, in addition, when there is a choice of multiple APs, the AP with the strongest signal is selected. The comparisons are presented in terms of overall system battery lifetime averaged over all MNs and distributedness of load among the attachment points (i.e., APs and BSs).

As stated earlier, for a given set of loads and MNs' battery lifetimes, the values of $\alpha$ and $\beta$ in solving the joint optimization problem in Eqs. (16) and (17) can be selected appropriately to put different emphases on battery lifetime and load balancing. The values of the weights, $\alpha$ and $\beta$, would be typically supplied by the network operator or carrier responsible for maintenance of the network. For instance, VHDCs for a region covering one or multiple APs and/or BSs can have algorithms that determine the values of the weights after obtaining the user profiles via the MIHF as addressed in Section II and then process them based on the network operator's policy [25]. For this study, based on some preliminary simulation runs with typical system and load parameters, we have determined that the first term in Eq. (16) (corresponding to battery lifetime) is typically about 5 orders of magnitude greater than the second term (corresponding to normalized load). This is naturally dependent on the measurement units used as well for each of the terms. Hence, for the joint optimization to work meaningfully, we must select $\beta$ values to be in the ballpark of $10^5$ times higher than those of $\alpha$, and vary each in its respective range to study performance sensitivity to their values.

The $95^{th}$-percentile confidence intervals for the measurement results (battery lifetime and load) reported here are within $\pm 1\%$ of the average based on 10 simulation runs. Figs. 8 and 9 show the percentage remaining battery lifetime averaged over all MNs, at the end of the simulation run (i.e., at 10,000 s) for the two

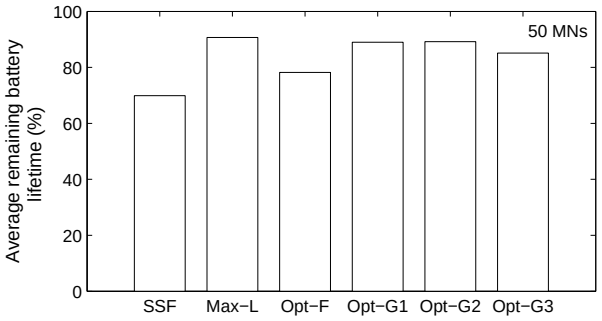


Fig. 8. Average remaining battery lifetime for the test case with 50 MNs.

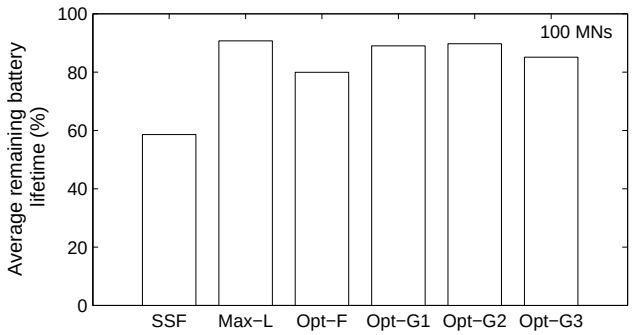


Fig. 9. Average remaining battery lifetime for the test case with 100 MNs.

test cases (50 and 100 MNs, respectively) for various optimization methods. In these plots, 100 % corresponds to the remaining battery lifetime at he beginning of the simulation. These methods include solving the battery lifetime optimization problem, **Max-**$L$, the load fairness optimization problem, **Opt-**$F$, and the joint optimization problem, **Opt-**$G$. For the joint optimization function, **Opt-**$G$, $\alpha$ and $\beta$ are set such that $\frac{\beta}{\alpha}$=$10^5$, $3 \times 10^5$, and $5 \times 10^5$, which are denoted as **Opt-**$G1$, **Opt-**$G2$, and **Opt-**$G3$, respectively, in Figs. 8-13. As we would expect, **Max-**$L$ achieves the longest battery lifetime among all the cost functions or optimization methods in consideration (see Figs. 8 and 9). The SSF method connects MNs to an available attachment point based on the strongest signal criterion only, and hence performs the worst in terms of battery life usage.

In Figs. 10 and 11, we plot the percentage remaining battery lifetime averaged over all MNs versus simulation time for the two test cases of 50 MNs and 100 MNs, respectively. We observe the same phenomenon as in Figs. 8 and 9. The battery lifetime for all the four schemes decreases with time. However, **Max-**$L$ achieves the best performance in terms of average remaining battery lifetime, while SSF performs the worst. In Figs. 12 and 13, we plot the Coefficient of Variation (CoV) of

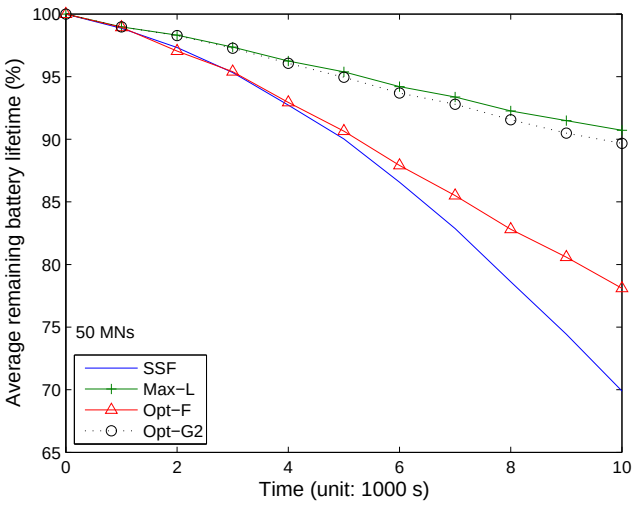


Fig. 10. Average remaining battery lifetime versus time when there are 2 BSs, 5 APs and 50 MNs.

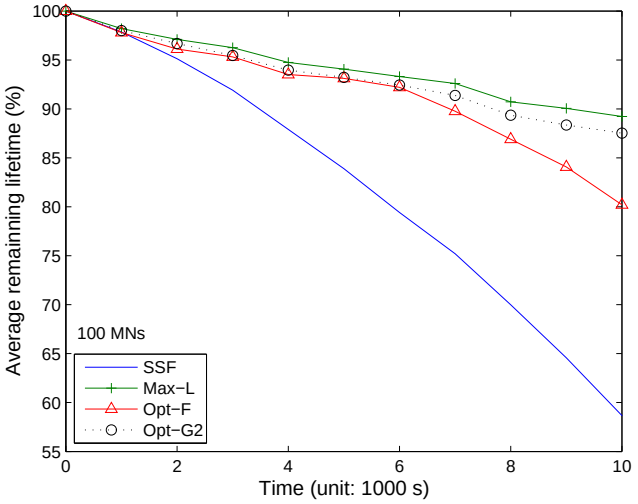


Fig. 11. Average remaining battery lifetime versus time when there are 2 BSs, 5 APs and 100 MNs.

loads which is defined as the standard deviation of loads observed at the APs divided by the mean load. This definition has been used extensively as a fairness metric in the literature for illustration of the distributedness of load (i.e., load balancing) [23]. Figs. 12 and 13 show that **Opt-**$F$ performs best among all the optimization methods as expected because **Opt-**$F$ aims to evenly distribute the load among attachment points accessible by MNs in a cellular coverage area. However, for **Opt-**$F$ method, the average battery lifetime is shorter compared to those for **Max-**$L$, **Opt-**$G1$, **Opt-**$G2$, and **Opt-**$G3$ as was noted in Figs. 8 and 9. SSF achieves the worst performance in terms of distributedness of load as well as battery lifetime. The weighted combined optimization method, **Opt-**$G$ provides performance that lies in

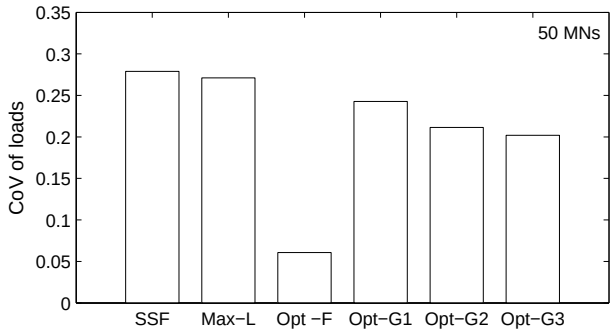


Fig. 12. Distributedness of load across attachment points when there are 50 MNs.

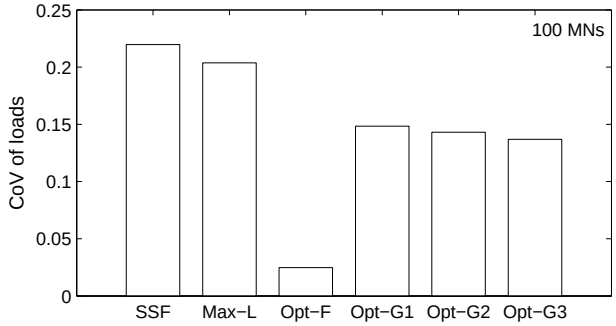


Fig. 13. Distributedness of load across attachment points when there are 100 MNs.

between those for **Max-**$L$ and **Opt-**$F$ in terms of either of the two performance metrics, i.e., battery lifetime or load fairness. In Figs. 14-17, we plot the overall load at each AP and each BS versus simulation time for the first test case with 50 MNs active in the test coverage area. Similarly, the overall load for the second test case with 100 active MNs are plotted in Figs. 18-21. These figures show how the load is distributed among APs and BSs by the proposed cost functions as well as the SSF approach during the entire simulation time. The detailed load distribution data corresponding to these Figures are given in Tables III- VIII in Appendix B. As mentioned in Section III, it is known that the bandwidth price level for WLANs is cheaper than that for cellular networks. Thus, in our simulation tests, $w_c$ is relatively larger than $w_a$ so that APs are selected in preference to BSs when an attachment point needs to be selected. That is, we aim to use cheaper WLAN bandwidth (especially, for multimedia traffic) in preference to the BS bandwidth. Through our proposed joint optimization method, the VHDC has the flexibility to manipulate the relative emphasis on extending battery lifetime vs. load balancing. We observe from Fig. 14 that under the SSF scheme, one of the five APs (AP4 in the graph) carries the maximum load of 1664 kbps at the simulation unit time 6000s and the maximum load of 2304 kbps is

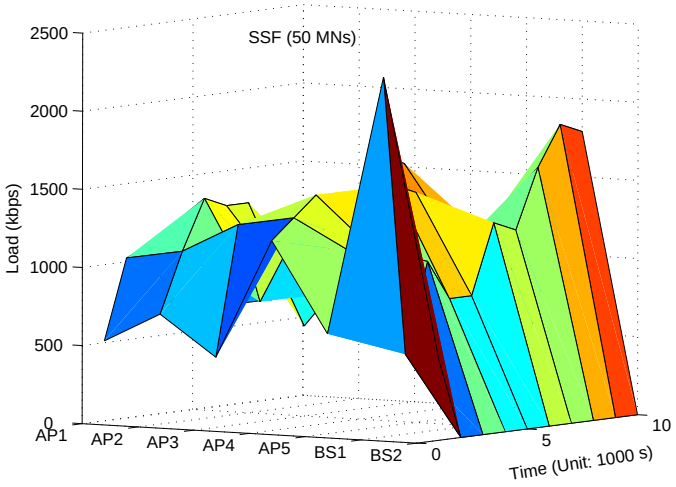


Fig. 14. Load status (kbps) at APs and BSs versus simulation time for SSF method when there are 50 MNs.

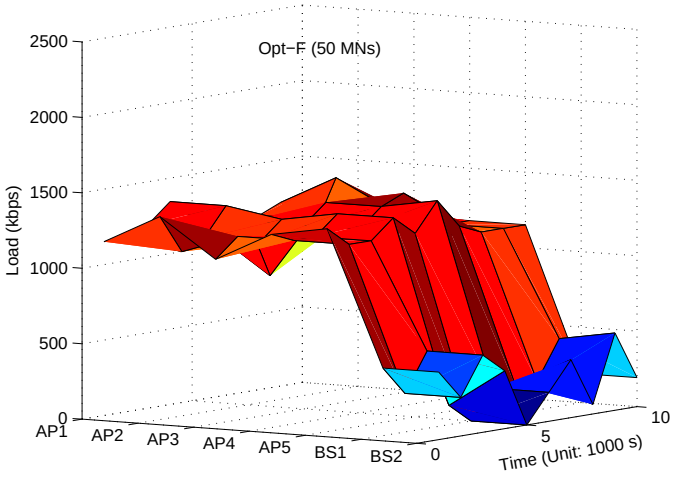


Fig. 16. Load status (kbps) at APs and BSs versus simulation time for **Opt-**$F$ method when there are 50 MNs.

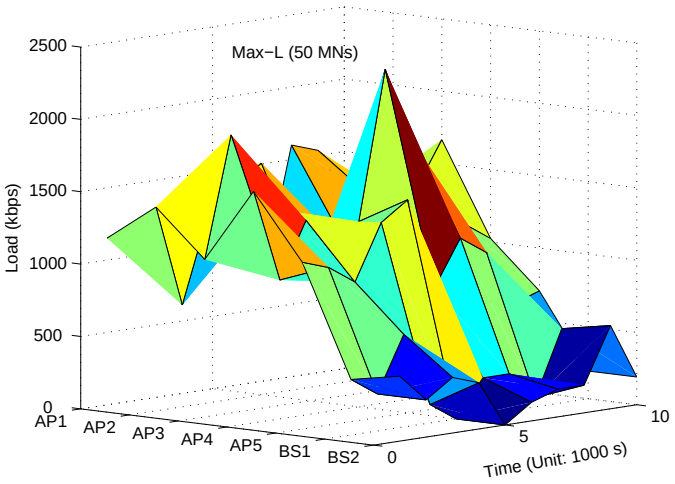


Fig. 15. Load status (kbps) at APs versus simulation time for **Max-**$L$ method when there are 50 MNs.

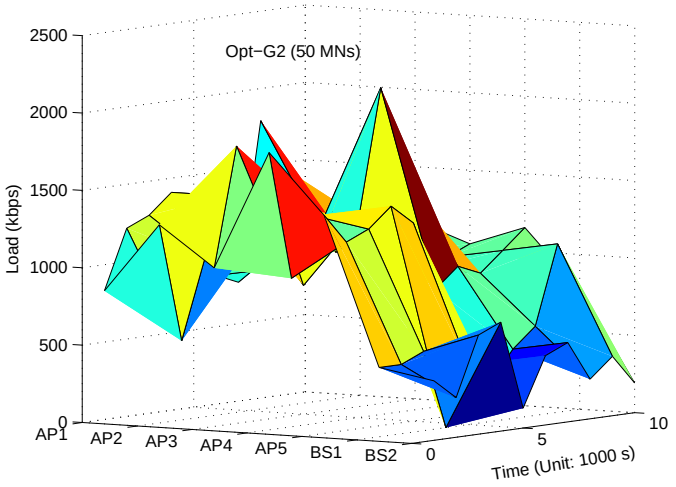


Fig. 17. Load status (kbps) at APs and BSs versus simulation time for **Opt-**$G2$ method when there are 50 MNs.

associated with one BS (BS1) at the time 1000s. We observe the SSF method does a poor job of not only distributing the load very unevenly across APs but also it favors BS1 at the expense of BS2 in the simulation test case with 50 MNs. For the **Opt-**$F$ method, the load is quite evenly distributed over the APs mostly within an approximate narrow range of 1088-1408 kbps, as seen in Fig. 16. The data corresponding to Fig. 16 is shown in Table III in Appendix B. Similar observations can be made for the test case with 100 MNs from the plots shown in Figs. 18 and 20. Based on the two sets of plots shown in Figs. 12-15 and Figs. 16-19, the following two other important observations can be made about the advantages of our proposed methods **Max-**$L$, **Opt-**$F$, and Max $G(\mathbf{X}, \alpha, \beta)$ over the SSF method: (1) These methods show lower preference for BSs over APs which is desirable since APs are better suited to carry higher-bandwidth multi-media calls, and (2) The parameters $\alpha$ and $\beta$ can be suitably tuned by the network operator to achieve pure load balancing optimization or pure battery lifetime optimization or a suitable weighted combination of the two.

### *C. Battery Lifetime Results for Heterogeneous Networks Including Ad Hoc Mode*

In this subsection, we compare the performance of the proposed route selection algorithm which is described in Section IV with that of DSR. The results presented here are obtained from the simulation model described

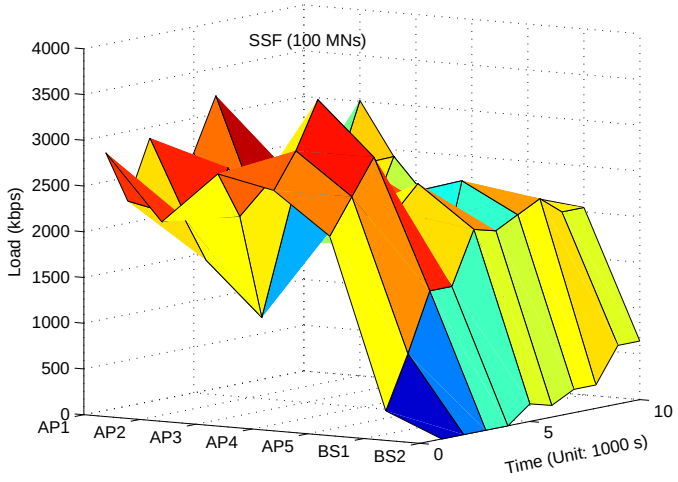


Fig. 18. Load status (kbps) at APs and BSs versus simulation time for SSF method when there are 100 MNs.

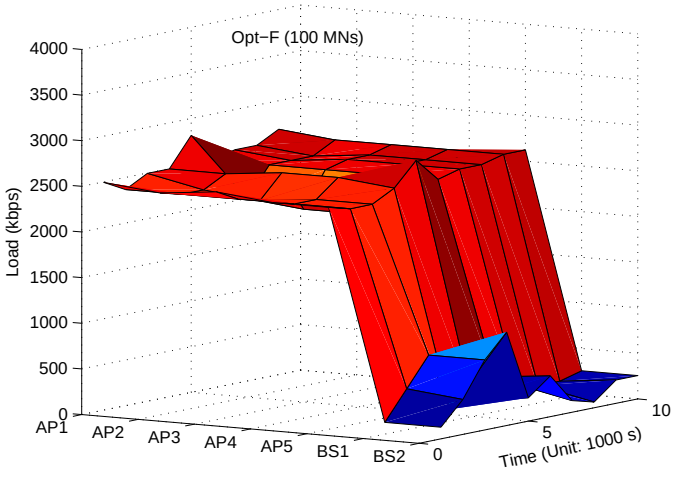


Fig. 20. Load status (kbps) at APs and BSs versus simulation time for **Opt-**$F$ method when there are 100 MNs.

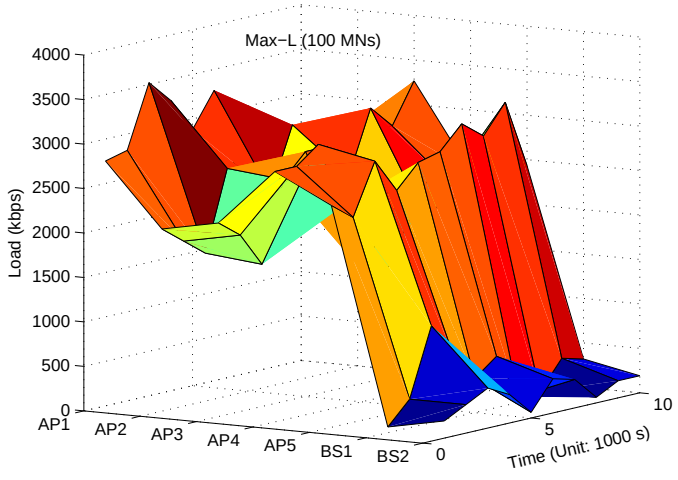


Fig. 19. Load status (kbps) at APs and BSs versus simulation time for **Max-**$L$ method when there are 100 MNs.

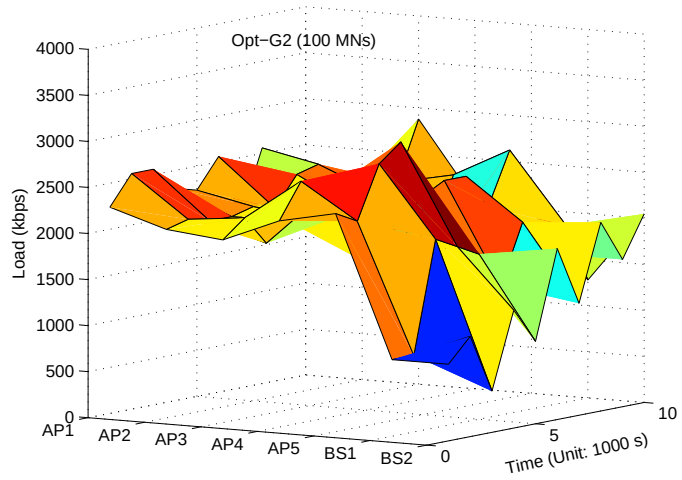


Fig. 21. Load status (kbps) at APs and BSs versus simulation time for **Opt-**$G2$ method when there are 100 MNs.

in Section V-A (see Fig. 6 (b)), wherein the number of MNs in an ad hoc area is set to 40. As shown in Fig. 6 (b), the MNs operating in ad hoc mode are not within the coverage of any AP or BS, but are in range of each other via their short-range radios. This figure also shows two example routes from a source node (i.e., ad hoc mode MN) to two candidate proxy nodes; proxy node 1 reaches the destination via an AP and proxy node 2 does the same via a BS. The route selection algorithm, $r_{max}$, proposed in Section IV may typically select a different route than that selected by DSR algorithm, because our $r_{max}$ algorithm is enhanced to take into account the battery lifetimes of MNs in the route.

In our simulation runs, a pair of nodes consisting of one each in the ad hoc and cellular coverage areas are selected randomly as the source and destination nodes, respectively. Five such pairs of nodes are selected per 1000s of time, and one connection is generated each time. All the MNs are randomly distributed and move randomly. When they move, a new route is selected between the pair of nodes if the current route becomes unusable due to the movement and power considerations. The amount of data sent per connection from the source node is exponentially distributed with mean $D$ Kbytes per connection. $D$ is set to one of these three values: 5, 10, and 15 Kbytes. The initial battery power of each MN is 1000 mJ. We use the power consumption model developed in [24] for the WLAN interface, where the energy consumed by a network interface as it sends and receives point-to-point messages, is described as $0.8$mJ$+$

TABLE II

(A) THE REMAINING ENERGY (MJ) OF EACH PROXY NODE AFTER 20,000S OF SIMULATION TIME, AND (B) THE AVERAGE CVE FOR THE PROXY NODES, MEASURED AT 1000S INTERVALS AND AVERAGED OVER SIMULATION TIME (THE $95^{th}$-PERCENTILE CONFIDENCE INTERVALS FOR THE MEASUREMENTS REPORTED IN THIS TABLE ARE WITHIN $\pm 1\%$ OF THE AVERAGE BASED ON 10 SIMULATION RUNS.)

(a) Remaining energy (mJ) of each proxy node

| $D = 5$ | | | |
|---|---|---|---|
| | Proxy 1 | Proxy 2 | Proxy 3 |
| DSR | 743.3 | 1000 | 1000 |
| $r_{max}$ | 913.8 | 910.3 | 919.3 |
| $D = 10$ | | | |
| | Proxy 1 | Proxy 2 | Proxy 3 |
| DSR | 456.8 | 1000 | 1000 |
| $r_{max}$ | 812.4 | 806.4 | 838 |
| $D = 15$ | | | |
| | Proxy 1 | Proxy 2 | Proxy 3 |
| DSR | 254 | 1000 | 1000 |
| $r_{max}$ | 702.6 | 783.5 | 768 |

(b) Average CVE

| $D$ | 5 | 10 | 15 |
|---|---|---|---|
| DSR | 0.08 | 0.18 | 0.27 |
| $r_{max}$ | 0.018 | 0.043 | 0.077 |
| $\frac{\text{CVE of DSR}}{\text{CVE of } r_{max}}$ | 4.44 | 4.19 | 3.51 |

2.4mJ/Kbyte $\times$ $D$. Ten independent simulation runs of duration 20,000s each are performed, measurements are taken at intervals of 1000s, and the results reported are averaged over the ten runs.

Here our focus is on the power consumed by proxy nodes while forwarding packets on behalf of other nodes in the ad hoc area. The proposed algorithm, $r_{max}$, aims to improve the longevity of the network by making the battery life for proxy MNs last longer. Accordingly, in this algorithm the load gets balanced over all accessible proxy nodes so that MNs in the ad hoc area would be able to sustain connectivity for longer period with MNs outside the ad hoc area. The performance of our proposed $r_{max}$ algorithm and that of DSR are compared in Table II. The $95^{th}$ percentile confidence intervals for the measurements reported in this table are within $\pm 1\%$ of the average based on ten independent simulation runs. This table compares the two algorithms using two separate metrics: (1) The remaining energy of each of the three available proxy nodes at the end of simulation run length of 20,000s, and (2) The covariance of remaining energy, $CVE$, for the three proxy nodes (measured at intervals of 1000s and averaged over the simulation run). It is evident that the $r_{max}$ algorithm performs consistently better than DSR. As an example, in Table II-(a) we see that for the case of D = 15 Kbytes, the remaining energy of Proxy 1 is 254 mJ and 702.6 mJ, respectively, for the DSR and $r_{max}$ algorithms. This effectively means that the probability that Proxy 1 MN will shut off is much higher for DSR as compared to that for the $r_{max}$ algorithm. In essence, the proposed $r_{max}$ algorithm distributes the load evenly across the three proxy MNs so that each has about equal remaining energy. This is further illustrated in Table II-(b) and Fig. 22 by comparing the $CVE$ values for DSR and $r_{max}$ algorithms. The improvement in $CVE$ values for the $r_{max}$ algorithm over DSR are quite significant, and are lower by factors of 4.44, 4.19, and 3.51 for the cases of $D$ = 5, 10, and 15 Kbytes, respectively.

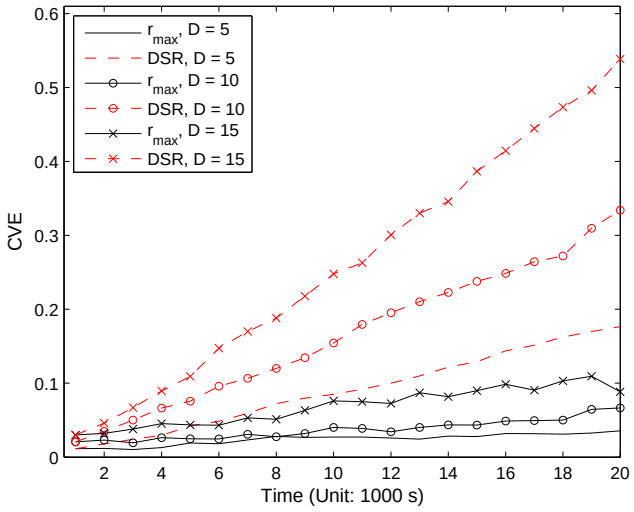


Fig. 22. CVE for the remaining energy of the three proxy nodes in the heterogeneous network including ad hoc mode.

## VI. CONCLUSION

When connections need to migrate between heterogeneous networks for performance and high-availability reasons, then seamless vertical handoff is a necessary first step. In the near future, vehicular and other mobile applications will expect seamless vertical handoff between heterogeneous access networks, which will include WLANs, cellular networks (UMTS, CDMA2000), Wi-MAX and VANETs/MANETs.

New metrics for vertical handoff continue to emerge and the use of new metrics make the vertical handoff decision process increasingly more complex. In this paper, we tried to highlight the metrics best suited for the vertical handoff decisions. We also proposed a generalized vertical handoff decision algorithm that seeks to optimize a combined cost function involving battery lifetime of MNs and load balancing over APs/BSs. We further proposed an enhanced algorithm for the case

when ad hoc mode MNs forming VANET/MANET are included in the heterogeneous networks. This latter algorithm allows the proxy nodes, which provide connectivity to the nearest AP or BS for the ad hoc mode MNs, to share transit loads with the goal of balancing their consumption of battery power. Our performance results based on detailed simulations illustrate that the proposed algorithms perform much better than the conventional optimization based on the SSF method, which is based on RSS alone. Our proposed method gives the network operator the leverage to easily vary the emphasis from maximizing the overall system battery lifetime for MNs to seeking fairness of load distribution over APs and BSs, with weighted combinations in-between.

## REFERENCES


[1] 3GPP TR 23.234 v7.1.0, "3GPP System to WLAN Interworking; System Description (Release 7)," March 2006, http://www.3gpp.org/specs/specs.htm.

[2] A.K. Salkintzis, "Internetworking Techniques and Architectures for WLAN/3G Integration Toward 4G Mobile Data Networks," *IEEE Wireless Communications Magazine*, vol. 11, no. 3, pp. 50-61, June 2004.

[3] M. Buddhikot, G. Chandranmenon, S. Han, Y. W. Lee, S. Miller, and L. Salgarellim, "Integration of 802.11 and Third-Generation Wireless Data Networks," *IEEE Infocom'03*, vol. 1, pp. 503-512, San Francisco, USA, March 2003.

[4] V. Varma, S. Ramesh, K. Wong, and J. Friedhoffer, "Mobility Management in Integrated UMTS/WLAN Networks", *IEEE ICC'03*, vol. 2 pp. 1048-1053, Ottawa, Canada, May 2003.

[5] T.B. Zahariadis, "Guest Editorial: Migration toward 4G Wireless Communications," *IEEE Wireless Communications Magazine*, vol. 11, no. 3, pp. 6-7, June 2004.

[6] J. McNair and F. Zhu, "Vertical Handoffs in Fourth-Generation Multinetwork Environments," *IEEE Wireless Communications Magazine*, vol. 11, no. 3, pp. 8-15, June 2004.

[7] Chuanxiong Guo, Zihua Guo, Qian Zhang and Wenwu Zhu, "A Seamless and Proactive End-to-End Mobility Solution for Roaming across Heterogeneous Wireless Networks", *IEEE Journal on Selected Areas in Communications*, vol. 22, no. 5, pp. 834-848, June 2004.

[8] R. Chakravorty, P. Vidales, K. Subramanian, I. Pratt, and J. Crowcroft, "Performance Issues with Vertical Handovers - Experiences from GPRS Cellular and WLAN Hot-spots Integration," *IEEE Percom'04: Pervasive Computing and Communications*, Orlando, FL, USA, March 2004.

[9] N. Nasser, A. Hasswa, and H. Hassanein, "Handoffs in Fourth Generation Heterogeneous Networks," *IEEE Communications Magazine*, vol. 44, no. 10, pp. 96-103, October 2006.

[10] "IEEE 802.21 Standard and Metropolitan Area Networks: Media Independent Handover Services," Draft P802.21/D00.05, January 2006.

[11] H. Wu, C. Qiao, S. De, and O. Tonguz, "Integrated Cellular and Ad Hoc Relaying Systems: iCAR," *IEEE Journal on Selected Areas in Communications*, vol. 19, no. 10, pp. 2105-2115, October 2001.

[12] D. Cavalcanti, D. Agrawal, C. Corderio, B. Xie and A. Kumar "Issues in Ingetrating Cellular Networks, WLANs, and MANETs: A Futuristic Heterogeneous Wireless Network," *IEEE Wireless Communcations Magazine*, vol. 12, no. 3, pp. 30-41, June 2005.

[13] A. Dutta, S. Das, D. Famolari, Y. Ohba, K. Taniuchi, T. Kodama, and H. Schulzrinne. "Seamless Handoff across Heterogeneous Networks - An 802.21 Centric Approach," *IEEE WPMC'05: Wireless Personal Multimedia Communications*, Aalborg, Denmark, September 2005.

[14] *NIST Seamless and Secure Mobility Project* Available: http://www.antd.nist.gov/seamlessandsecure.shtml#project.

[15] S.J. Yoo, D. Cypher, and N. Golmie, "LMS Predictive Link Triggering for Seamless Handovers in Heterogeneous Wireless Networks," *Proceedings of MILCOM 2007*, Orlando Florida, October 28-30, 2007.

[16] G. Lampropoulos, A.K. Salkintzis, and N. Passas, "Media-Independent Handover for Seamless Service Provision in Heterogeneous Networks," *IEEE Communications Magazine*, vol. 46, no. 1, pp. 64-71, January 2008.

[17] H. Zhai, J. Wang and Y. Fang, "Providing Statistical QoS Guarantee for Voice over IP in the IEEE 802.11 Wireless LANs," *IEEE Wireless Communications Magazine*, vol.13, no.1, pp.36-43, February 2006.

[18] H. Zhai, X. Chen, and Y. Fang, "A Call Admission and Rate Control Scheme for Multimedia Support over IEEE 802.11 Wireless LANs," *Wireless Networks*, vol. 12, no. 4, pp. 451-463, July 2006.

[19] D. Johnson, D. Maltz, and Y. Hu, "The Dynamic Source Routing Protocol for Mobile Ad Hoc Networks (DSR)," *Internet Draft*, draft-ietf-manet-dsr-10.txt, July 2004.

[20] H. Luo, R. Ramjee, P. Sinha, L. Li, and S. Lu, "UCAN: A Unified Cellular and Ad-Hoc Network Architecture," *ACM Mobicom'03*, pp. 353-367, San Diego, CA, USA, September 2003.

[21] R. Fletcher and S. Leyffer, "Numerical Experience with Lower Bounds for MIQP Branch-And-Bound," *SIAM Journal on Optimization*, vol. 8, no. 2, pp. 604-616, 1998.

[22] TOMLAB: A General Purpose MATLAB Environment for Optimization, http://tomlab.biz.com

[23] R. Jain, "The Art of Computer Systems Performance Analysis: Techniques for Experimental Design, Measurement, Simulation, and Modeling," *Wiley-Interscience*, New York, NY, April 1991.

[24] L. Feeney and M. Nilsson, "Investigating the Energy Consumption of a Wireless Network Interface in an Ad Hoc Networking Environment," *IEEE Infocom'01*, vol.3, pp. 1548-1557, Anchorage, AK, USA, 2001.

[25] K.P. Demestichas, A. Koutsorodi, E. Adamopoulou, and M. Theologou, "Modelling User Preferences and Configuring Services in B3G Devices," *Wireless Networks*, Published online, July 2007.

## APPENDIX A

In order to take into account the fairness of load distribution, a simple but useful lemma is provided as follows:

LEMMA 1 *Let* $\{b_i\}_{i=1}^{I}$ *be a finite sequence of real numbers and* $A = \frac{1}{I}\sum_{i=1}^{I} b_i$ *the mean value of the sequence. Then,*

$$\sum_{i=1}^{I} b_i^2 = \sum_{i=1}^{I}(b_i - A)^2 + IA^2. \tag{21}$$

PROOF. Since $\sum_{i=1}^{I}(b_i - A) = 0$,

$$\begin{aligned}\sum_{i=1}^{I} b_i^2 &= \sum_{i=1}^{I}[(b_i - A) + A]^2 \\ &= \sum_{i=1}^{I}[(b_i - A)^2 + 2A(b_i - A) + A^2] \\ &= \sum_{i=1}^{I}(b_i - A)^2 + 2A\sum_{i=1}^{I}(b_i - A) + \sum_{i=1}^{I} A^2 \\ &= \sum_{i=1}^{I}(b_i - A)^2 + IA^2.\end{aligned} \tag{22}$$

## APPENDIX B

TABLE III

FOR SSF AND **MAX-$L$**, LOAD STATUS (KBPS) AT APS AND BSS DURING SIMULATION WHEN THERE ARE 2 BSS, 5 APS AND 50 MNS (TIME UNIT: 1000S)

| Time | SSF (50-node) | | | | | | | **Max-$L$** (50-node) | | | | | | |
|---|---|---|---|---|---|---|---|---|---|---|---|---|---|---|
| | AP1 | AP2 | AP3 | AP4 | AP5 | BS1 | BS2 | AP1 | AP2 | AP3 | AP4 | AP5 | BS1 | BS2 |
| 1 | 512 | 704 | 448 | 1216 | 640 | 2304 | 512 | 1152 | 1408 | 1088 | 1600 | 1152 | 384 | 448 |
| 2 | 1024 | 1088 | 1280 | 1344 | 1152 | 512 | 0 | 1216 | 704 | 1920 | 960 | 1088 | 256 | 256 |
| 3 | 1088 | 1408 | 768 | 1472 | 1152 | 1088 | 0 | 1280 | 1088 | 1344 | 1344 | 960 | 640 | 384 |
| 4 | 704 | 1344 | 896 | 832 | 1536 | 832 | 0 | 1408 | 1472 | 1344 | 1088 | 1344 | 128 | 320 |
| 5 | 1024 | 1344 | 576 | 1024 | 1472 | 832 | 0 | 1088 | 1600 | 832 | 1280 | 1472 | 0 | 0 |
| 6 | 768 | 704 | 832 | 1664 | 1152 | 1280 | 0 | 832 | 896 | 1088 | 2304 | 832 | 256 | 128 |
| 7 | 640 | 896 | 1024 | 1600 | 1088 | 1216 | 0 | 768 | 1088 | 1216 | 1792 | 1152 | 256 | 192 |
| 8 | 640 | 960 | 1088 | 896 | 1152 | 1600 | 0 | 1600 | 1024 | 1088 | 1024 | 1024 | 64 | 192 |
| 9 | 768 | 1024 | 1152 | 1024 | 768 | 1856 | 0 | 1536 | 1280 | 1344 | 1152 | 640 | 512 | 576 |
| 10 | 896 | 896 | 640 | 1024 | 384 | 1792 | 0 | 1216 | 1216 | 1664 | 1024 | 704 | 192 | 192 |

TABLE IV

FOR **OPT-$F$** AND **OPT-$G1$**, LOAD STATUS (KBPS) AT APS AND BSS DURING SIMULATION WHEN THERE ARE 2 BSS, 5 APS AND 50 MNS (TIME UNIT: 1000S)

| Time | **Opt-$F$** (50-node) | | | | | | | **Opt-$G1$** (50-node) | | | | | | |
|---|---|---|---|---|---|---|---|---|---|---|---|---|---|---|
| | AP1 | AP2 | AP3 | AP4 | AP5 | BS1 | BS2 | AP1 | AP2 | AP3 | AP4 | AP5 | BS1 | BS2 |
| 1 | 1152 | 1344 | 1088 | 1280 | 1344 | 448 | 448 | 832 | 1344 | 1024 | 1728 | 1408 | 448 | 384 |
| 2 | 1152 | 1088 | 1216 | 1216 | 1216 | 256 | 256 | 1216 | 512 | 1792 | 960 | 1216 | 448 | 256 |
| 3 | 1216 | 1152 | 1152 | 1216 | 1216 | 512 | 512 | 1280 | 1024 | 1216 | 1344 | 1280 | 512 | 640 |
| 4 | 1344 | 1344 | 1280 | 1344 | 1344 | 128 | 384 | 1408 | 1408 | 1280 | 1088 | 1408 | 0 | 704 |
| 5 | 1216 | 1216 | 1216 | 1216 | 1216 | 0 | 0 | 1088 | 1472 | 832 | 1280 | 1280 | 192 | 0 |
| 6 | 1088 | 832 | 1344 | 1344 | 1408 | 192 | 192 | 704 | 896 | 1280 | 2112 | 832 | 64 | 512 |
| 7 | 1152 | 1216 | 1216 | 1408 | 1216 | 192 | 384 | 768 | 1088 | 1216 | 1536 | 1152 | 256 | 704 |
| 8 | 1152 | 1088 | 1152 | 1088 | 1152 | 192 | 64 | 1792 | 1024 | 1088 | 896 | 1088 | 384 | 256 |
| 9 | 1216 | 1408 | 1216 | 1152 | 1152 | 448 | 512 | 1664 | 1280 | 1152 | 960 | 640 | 896 | 384 |
| 10 | 1088 | 1088 | 1152 | 1152 | 1152 | 192 | 192 | 1152 | 1216 | 1344 | 1024 | 832 | 576 | 192 |

TABLE V

FOR **OPT-$G2$** AND **OPT-$G3$**, LOAD STATUS (KBPS) AT APS AND BSS DURING SIMULATION WHEN THERE ARE 2 BSS, 5 APS AND 50 MNS (TIME UNIT: 1000S)

| Time | **Opt-$G2$** (50-node) | | | | | | | **Opt-$G3$** (50-node) | | | | | | |
|---|---|---|---|---|---|---|---|---|---|---|---|---|---|---|
| | AP1 | AP2 | AP3 | AP4 | AP5 | BS1 | BS2 | AP1 | AP2 | AP3 | AP4 | AP5 | BS1 | BS2 |
| 1 | 832 | 1280 | 1024 | 1792 | 1408 | 448 | 384 | 832 | 1088 | 1152 | 1472 | 1472 | 832 | 832 |
| 2 | 1216 | 512 | 1792 | 960 | 1216 | 448 | 256 | 1216 | 512 | 1792 | 960 | 1088 | 576 | 256 |
| 3 | 1280 | 1024 | 1216 | 1344 | 1280 | 512 | 640 | 1280 | 1216 | 1216 | 1152 | 1280 | 576 | 640 |
| 4 | 1408 | 1408 | 1280 | 1088 | 1408 | 0 | 704 | 1408 | 1408 | 1280 | 1088 | 1408 | 0 | 704 |
| 5 | 896 | 1344 | 832 | 1280 | 1280 | 384 | 128 | 896 | 1344 | 832 | 1280 | 1280 | 384 | 128 |
| 6 | 832 | 896 | 1280 | 2112 | 832 | 256 | 448 | 832 | 896 | 1664 | 1728 | 832 | 256 | 448 |
| 7 | 768 | 1088 | 1280 | 1472 | 960 | 448 | 512 | 768 | 1024 | 1344 | 1472 | 960 | 512 | 512 |
| 8 | 1792 | 1152 | 1024 | 896 | 896 | 576 | 256 | 1792 | 1280 | 960 | 896 | 896 | 640 | 256 |
| 9 | 1472 | 1088 | 960 | 960 | 1024 | 1088 | 384 | 1472 | 960 | 960 | 960 | 832 | 1408 | 384 |
| 10 | 1088 | 1152 | 1152 | 1024 | 1152 | 768 | 192 | 1088 | 1152 | 1024 | 1152 | 1152 | 1088 | 192 |

TABLE VI

FOR SSF AND **MAX-$L$**, LOAD STATUS (KBPS) AT APS AND BSS DURING SIMULATION WHEN THERE ARE 2 BSS, 5 APS AND 100 MNS (TIME UNIT: 1000S)

| Time | SSF (100-node) | | | | | | | **Max-$L$** (100-node) | | | | | | |
|---|---|---|---|---|---|---|---|---|---|---|---|---|---|---|
| | AP1 | AP2 | AP3 | AP4 | AP5 | BS1 | BS2 | AP1 | AP2 | AP3 | AP4 | AP5 | BS1 | BS2 |
| 1 | 2816 | 2112 | 2688 | 2560 | 2112 | 256 | 0 | 2752 | 2048 | 2176 | 2816 | 2496 | 64 | 192 |
| 2 | 2240 | 2112 | 2176 | 2944 | 2496 | 832 | 0 | 2816 | 1856 | 1984 | 2816 | 2304 | 320 | 320 |
| 3 | 2880 | 1600 | 1024 | 3456 | 2880 | 1472 | 0 | 3520 | 1664 | 1600 | 3008 | 2880 | 1088 | 448 |
| 4 | 2240 | 2560 | 1792 | 2112 | 2240 | 1472 | 0 | 3264 | 2560 | 2496 | 2240 | 2496 | 704 | 320 |
| 5 | 2624 | 1344 | 1920 | 1792 | 2496 | 2048 | 192 | 2880 | 1856 | 2752 | 1472 | 2752 | 384 | 64 |
| 6 | 3200 | 1600 | 2752 | 1344 | 1408 | 1984 | 128 | 3264 | 2176 | 2752 | 1344 | 2816 | 576 | 384 |
| 7 | 2240 | 2304 | 1920 | 2240 | 2432 | 2112 | 256 | 2304 | 2880 | 2368 | 2048 | 3072 | 64 | 320 |
| 8 | 2240 | 2176 | 1920 | 2176 | 1856 | 2240 | 256 | 2304 | 2624 | 3072 | 1856 | 2880 | 64 | 64 |
| 9 | 1664 | 2304 | 2496 | 1792 | 2176 | 2048 | 640 | 2304 | 2624 | 2816 | 2240 | 3200 | 384 | 192 |
| 10 | 1216 | 3008 | 2048 | 1408 | 2112 | 2048 | 640 | 1856 | 2560 | 3264 | 2304 | 2432 | 320 | 192 |

TABLE VII

FOR **OPT-$F$** AND **OPT-$G1$**, LOAD STATUS (KBPS) AT APS AND BSS DURING SIMULATION WHEN THERE ARE 2 BSS, 5 APS AND 100 MNS (TIME UNIT: 1000S)

| Time | **Opt-$F$** (100-node) | | | | | | | **Opt-$G1$** (100-node) | | | | | | |
|---|---|---|---|---|---|---|---|---|---|---|---|---|---|---|
| | AP1 | AP2 | AP3 | AP4 | AP5 | BS1 | BS2 | AP1 | AP2 | AP3 | AP4 | AP5 | BS1 | BS2 |
| 1 | 2496 | 2432 | 2496 | 2432 | 2432 | 128 | 128 | 2496 | 2048 | 1984 | 2496 | 2496 | 576 | 448 |
| 2 | 2368 | 2368 | 2368 | 2368 | 2368 | 448 | 384 | 2560 | 2112 | 2176 | 2688 | 2304 | 576 | 768 |
| 3 | 2496 | 2368 | 2304 | 2368 | 2368 | 768 | 768 | 2688 | 2048 | 1664 | 2624 | 2688 | 2048 | 448 |
| 4 | 2496 | 2496 | 2560 | 2560 | 2496 | 128 | 1024 | 2432 | 2560 | 2240 | 2048 | 2752 | 1920 | 832 |
| 5 | 2816 | 2176 | 2112 | 2112 | 2752 | 192 | 256 | 2496 | 2240 | 2432 | 1664 | 2368 | 896 | 576 |
| 6 | 2496 | 2496 | 2496 | 2496 | 2496 | 384 | 448 | 2816 | 2112 | 2432 | 1792 | 2624 | 704 | 1216 |
| 7 | 2560 | 2496 | 2560 | 2560 | 2560 | 256 | 128 | 2048 | 2624 | 1984 | 2496 | 2688 | 960 | 768 |
| 8 | 2560 | 2496 | 2560 | 2560 | 2560 | 192 | 64 | 2240 | 2496 | 2432 | 1792 | 2432 | 960 | 1216 |
| 9 | 2688 | 2624 | 2624 | 2624 | 2624 | 192 | 256 | 2304 | 1920 | 2560 | 2688 | 2688 | 1280 | 704 |
| 10 | 2368 | 2496 | 2304 | 2368 | 2624 | 256 | 256 | 1856 | 2176 | 3072 | 2304 | 2240 | 704 | 1216 |

TABLE VIII

FOR **OPT-$G2$** AND **OPT-$G3$**, LOAD STATUS (KBPS) AT APS AND BSS DURING SIMULATION WHEN THERE ARE 2 BSS, 5 APS AND 100 MNS (TIME UNIT: 1000S)

| Time | **Opt-$G2$** (100-node) | | | | | | | **Opt-$G3$** (100-node) | | | | | | |
|---|---|---|---|---|---|---|---|---|---|---|---|---|---|---|
| | AP1 | AP2 | AP3 | AP4 | AP5 | BS1 | BS2 | AP1 | AP2 | AP3 | AP4 | AP5 | BS1 | BS2 |
| 1 | 2240 | 2048 | 1984 | 2240 | 2368 | 832 | 832 | 2048 | 1856 | 1984 | 2240 | 2176 | 1216 | 1024 |
| 2 | 2560 | 2112 | 2176 | 2624 | 2240 | 832 | 1088 | 2432 | 2304 | 2176 | 2624 | 2240 | 1024 | 1280 |
| 3 | 2560 | 2048 | 1856 | 2432 | 2816 | 2048 | 448 | 2304 | 2176 | 2176 | 2176 | 2816 | 2048 | 448 |
| 4 | 2304 | 2048 | 2048 | 2176 | 3008 | 1920 | 1280 | 2048 | 2048 | 1856 | 2112 | 2688 | 1856 | 2048 |
| 5 | 2240 | 2112 | 2048 | 1600 | 2368 | 1792 | 896 | 1984 | 2112 | 2048 | 1856 | 2240 | 1984 | 1536 |
| 6 | 2560 | 2048 | 2240 | 1600 | 2496 | 1408 | 1856 | 2368 | 1984 | 2368 | 1600 | 2496 | 1536 | 2048 |
| 7 | 1856 | 2368 | 2048 | 2112 | 2496 | 2048 | 1216 | 1792 | 2176 | 2176 | 2304 | 2496 | 2048 | 1344 |
| 8 | 2560 | 2432 | 2176 | 1472 | 2112 | 1664 | 2048 | 2560 | 2240 | 1984 | 1856 | 2112 | 1664 | 2048 |
| 9 | 2112 | 1984 | 2240 | 2368 | 2688 | 1920 | 1600 | 1856 | 2048 | 2240 | 2368 | 2688 | 2043 | 1536 |
| 10 | 1792 | 1984 | 2880 | 2048 | 1984 | 1280 | 2048 | 2240 | 2048 | 2624 | 1856 | 1984 | 1344 | 2048 |

**SuKyoung Lee** received her B.S., M.S. and Ph.D. degrees in Computer Science from Yonsei University, Seoul, Korea, in 1992, 1995, and 2000, respectively. From 2000 to 2003, she worked with the Advanced Networking Technologies Division at the National Institute of Standards and Technology (NIST) in Gaithersburg, Maryland, USA. She is currently an assistant professor in the Department of Computer Science at Yonsei University, Seoul, Korea. Her current research interests include wireless and mobile networks as well as optical data networking.

**Kotikalapudi Sriram** (S'80-M'82-SM'97-F'00) received the B.S. and M.S. degrees from the Indian Institute of Technology in Kanpur, India, and a Ph.D. degree from Syracuse University in New York, all in electrical engineering. He is currently a Senior Researcher in the Advanced Networking Technologies Division, National Institute of Standards and Technology (NIST), Gaithersburg, MD. From 1983 to 2001, he held various positions at Bell Laboratories - the innovations arm of Lucent Technologies and formerly that of AT&T. His titles at Bell Laboratories included Consulting Member of Technical Staff (approximately top 1% of engineers in 2001) and Distinguished Member of Technical Staff. He is a contributing author and a coeditor of *Cable Modems: Current Technologies and Applications* (Piscataway, NJ: IEEE Press, 1999). He holds 17 U.S. patents. He is a coinventor on a patent related to quality-of-service (QoS) management for VOIP that was recognized by the MIT Technology Review Magazine as one of five Killer Patents in 2004. He has published over 60 papers in various IEEE and other international journals and major conferences. His interests and responsibilities include performance modeling, network architecture, Internet routing protocol security and scalability, design of protocols and algorithms for multiservice broadband networks, voiceover-IP (VOIP), wireless access networks, IP/MPLS/ATM traffic controls, and hybrid fiber-coax networks. He is a Fellow of the IEEE.

**Kyungsoo Kim** Kyungsoo Kim received the B.S., M.S., and Ph.D. degrees in Mathematics from Korea Advanced Institute of Science and Technology (KAIST), Daejeon, Korea, in 1996, 1998, and 2003, respectively. From 2003 to 2006, he has worked as a postdoctoral researcher in the Impedance Imaging Research Center at Kyung Hee University, the BK21 Mathematical Sciences Division at Seoul National University, and the National Institute for Mathematical Sciences, Korea. He is currently a research professor in the Institute of Natural Sciences at Kyung Hee University, Yongin, Korea. His current research interests include network optimization and vehicular computing system as well as numerical analysis, optimization, and mathematical modeling.

**JongHyup Lee** JongHyup Lee received his M.S. degree in Computer Science from Yonsei University, Seoul, Korea, in 2004. He is currently working towards Ph.D. degree at Yonsei University. His research interests include wireless networks and key management.

**Yoon Hyuk Kim** Yoon Hyuk Kim received the B.S., M.S., and Ph.D. degrees in Mechanical Engineering from Korea Advanced Institute of Science and Technology (KAIST), Daejeon, Korea, in 1992, 1994, and 2000, respectively. From 2000 to 2002, he has worked at the Orthopaedic Biomechanics Laboratory, Johns Hopkins University in Baltimore, Maryland, USA. He is currently an assistant professor in the Department of Mechanical Engineering at Kyung Hee University, Yongin, Korea. His current research interests include network optimization and vehicular computing system as well as biomechanical and biomedical engineering.

**Nada Golmie** Nada Golmie received her Ph.D. in Computer Science from the University of Maryland at College Park. Since 1993, she has been a research engineer in the advanced networking technologies division at the National Institute of Standards and Technology (NIST). She is currently the manager of the high-speed network technologies group. Her research in media access control and protocols for wireless networks led to over 100 papers presented at professional conferences, journals, and contributed to international standard organizations and industry led consortia. She is the author of Coexistence in Wireless Networks: Challenges and System-Level Solutions in the Unlicensed Bands (Cambridge University Press, 2006).